Stockholm University

# Bachelor Thesis

**Degree Project in Geology 15 hp**

# A Geochemical Investigation of a Potential Snowball Earth Sequence at Kapp Linné, Svalbard

Patrick Casey

Stockholm 2019

Department of Geological Sciences
Stockholm University
SE-106 91 Stockholm

# Content

Cover photo: A mother polar bear and her cubs inspecting the Kapp Linné diamictite.

## Abstract:

A geochemical analysis of the carbonates of the Kapp Linné formation of the Bellsund Group diamictites in SW Svalbard was conducted to attempt to place these formations into the framework of the "Snowball Earth" hypothesis and to correlate these formations with the Bellsund Group and Kapp Lyell diamictites to the south. Samples of carbonates were taken from three stratigraphic layers and the stable isotopes values of $\delta^{13}C$ and $\delta^{18}O$ were analyzed. Handheld XRF measurements were taken of their major oxide groups of each unit in the formation. Of the three carbonate layers identified two were clearly pre-glacial in origin based on their location below the diamictite. The third carbonate layer was interpreted as a "cap carbonate" situated above the diamictite.

The lowest pre-glacial unit had a $\delta^{13}C$ of +4.48‰, placing it within the standard pre-snowball Earth values. The carbonate unit directly under the diamictite had a $\delta^{13}C$ of -3‰, and the upper carbonate unit yielded $\delta^{13}C$ values of -2.5‰ to -3‰, falling within common values for a "cap carbonate" that is a key indicator of a snowball Earth deposit. XRF analysis of the layers immediately under and above the diamictite showed elevated levels of Fe and Mn. Increased levels of Fe and Mn are interpreted as signs of an anoxic ocean covered by ice for the millions of years of a snowball Earth. The similarity of the carbonate layer beneath the diamictite both lithologically and geochemically to a cap carbonate is hypothesized to be result of isolation of a depositional basin before sea levels rose and icebergs began to deposit ice-rafted debris as they melted.

The results show that the Kapp Linné formation correlates to the Bellsund Group, and the geochemical evidence is in line with the accepted "Snowball Earth" interpretation origin of the Bellsund Group diamictites.

## Introduction:

Neoproterozoic rocks of glacial origin have been found on every continent (Harland and Hambrey, 1981), evidence of a worldwide glacial event approximately 700 million years ago. Two major stages of Neoproterozoic glaciation have been identified and recent isotope dating has constrained their ages: the Sturtian glaciation (717-659Ma) and the Marinoan glaciation (645-635Ma) (Hoffman et al, 2017). These glaciations occurred during the Cryogenian period of the Neoproterozoic.

The Snowball Earth Hypothesis was proposed to explain widespread Neoproterozoic rocks of glacial origin. The origin of the Snowball Earth Hypothesis as a means of explaining Neoproterozoic glaciations was when Kirschvink (1992) measured the paleomagnetism of a Neoproterozoic glacial rock found in Australia which was determined to have been deposited at a low latitude (Kirschvink, 1992, Hoffman and Schrag, 2002). A low latitude glaciation would require extreme cooling of the planet and more evidence was needed to explain the cause of this cooling.

### Evidence leading to the Snowball Earth hypothesis:

Later work on Neoproterozoic glacial deposits showed that they were tied to carbonate deposits directly above glacial diamictites. These "cap carbonates" were unusual as they were tied to negative $\delta^{13}C$ excursions and are unique to the Neoproterozoic glaciations. They are found above glacial diamictites, and are believed to have formed when greenhouse conditions led to rapid ice melting in a high $CO_2$ environment which greatly increased the rate of chemical weathering bringing massive amounts of bicarbonate ions into the sea (Shields, 2005). The influx of bicarbonate as well as ocean-atmosphere carbon exchange led to massive precipitation of carbonate rock after the anoxia of a fully ice covered sea (Shields 2005, Hoffman *et al.*, 1998).

The anoxic conditions of the ocean stems from global sea ice cover preventing exchange of oxygen with ocean waters. Banded iron formations (BIF) have been found in the post glacial sediments of the Sturtian glaciation. BIF are common in the early geologic record from 3.7 Ga to 1.8 Ga and seldom seen after that period. BIF are tied to the first appearance of oxygen in the Earth's atmosphere when the earliest photosynthetic organisms evolved. Oxygen is a byproduct of photosynthesis, and oxygen in the atmosphere and ocean allowed free iron in the primordial oceans to oxidize and precipitate out, which formed iron rich rocks. Banded iron formations in the Snowball earth deposits have been put forward as evidence of an anoxic environment caused by global ice cover (Hoffman, 1998). Mid ocean rifting and hydrothermal activity added Fe to the system which was unable to react with oxygen until the melting of the sea ice allowed for exchange of oxygen with the oceans.

### Triggering a Snowball Earth:

The onset of a planet wide glaciation is likely to require numerous factors working in concert, and not just a single event (Schrag *et al*., 2002). Multiple models have been proposed for triggering a snowball Earth and most models agree that the paleogeography of the Neoproterozoic was a primary cause through ice-albedo feedback from cooling due to increased chemical weathering rates (Hoffman *et al*., 1998, Schrag *et al*., 2002). Albedo is the

measurement of the reflection of solar energy from the Earth back into space based on the reflectivity and heat absorption and retention of the surface. Lower albedo means that light will be readily absorbed, and not reflected back into space. Oceans have an albedo of approximately 0.06, while sand and rock have an albedo of approximately 0.4 and ice has an albedo of 0.55 (Henderdon-Sellers and Wilson, 1983) Prior to the first Cryogenian glaciation the continents were arranged as a single landmass in the lower latitudes named Rodinia (Fig. 1).

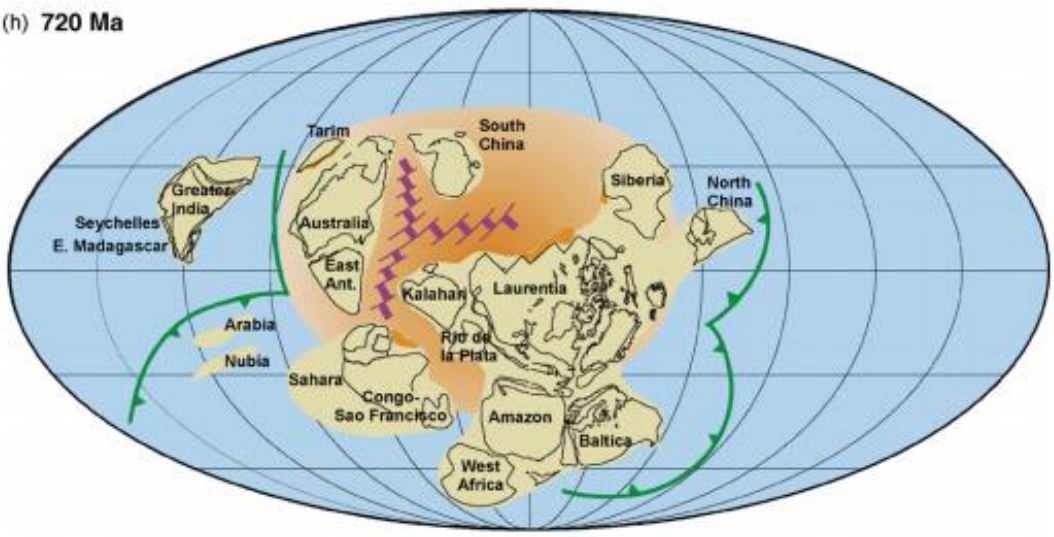


Fig. 1 The layout of the continents 720Ma. From Li et al. (2007)

A large landmass in the warmer tropics would lead to increased chemical weathering of carbonate and silicate rocks as rates of chemical weathering are determined by precipitation and temperature (Berner, 1978). The removal of $CO_2$ from the atmosphere would reduce global temperature and combined with high albedo from vegetation free continents at low latitudes this allowed the formation of low latitude ice caps.

Ice caps further reduce solar radiation forcing on the Earth's climate by reflecting sunlight away from the Earth. Insolation is highest at lower latitudes and decreases in higher latitudes. Ice caps at lower latitudes will therefore have a strong forcing effect on the amount of solar radiation being input into the earth system, which would lead to a negative feedback cycle. As lower latitude ice caps expand, there is less solar energy absorbed by the planet, which lowers temperatures, leading to further expansion of the ice caps. The expansion of the glaciers will lower sea level, and increase the landmass by exposing continental shelves, increasing planetary albedo and providing additional surface for weathering. This leads to yet lower temperatures until a runaway cooling has occurred, triggering planet-wide glaciations.

A model by Hyde et al. (2000) using the layout of Rodinia showed that even $pCO_2$ levels half that of modern levels of would allow for a runaway carbon drawdown through weathering, forming a snowball Earth.

## Global Meltdown:

Prior to the use of advanced computer models to simulate the conditions of a snowball Earth, it was believed that the Earth would never be able to recover from a total glaciation (Hoffman, 2017). Kirschvink (1992) proposed that the long duration of the glaciations allowed for volcanic $CO_2$ to build up in the atmosphere leading to a rapid meltdown of the glaciers. It was estimated by Caldiera and Kasting (1992) that to melt a fully glaciated planet the levels of atmospheric $pCO_2$ would need to reach 0.12 bar to overcome the effect of ice albedo of a planet-wide glaciation. Due to the complete shutdown of the hydrological cycle, traditional sinks for $CO_2$ such as carbonate/silicate weathering and atmosphere-sea interaction not remove $CO_2$ from the atmosphere, enabling this build up over millions of years of volcanic activity. The melting of an ice-covered Earth is estimated to have occurred within 10,000 years (Crowley *et al.*, 2001)

The melting of the glaciers and the opening of the anoxic seas lead to the strongest evidence of a global glacial event (Hoffman *et al.*, 1998; Hoffman and Schrag, 2002) through the formation of the previously discussed cap carbonate formations that directly overlie the glacial sediments. Cap carbonates sharply overlie sediments of glacial origin, and their wide distribution provides compelling evidence that the snowball Earth was global (Shields, 2005). Hoffman et al. (1998) first proposed cap carbonates as a reaction to the previously ice-covered oceans reacting with the $CO_2$ saturated atmosphere that triggered the greenhouse effect that melted the glaciers. Cap carbonates are typically meters to tens of meters thick and deposited over a period ranging from just hundreds to thousands of years due to the rapid rate at which the chemical conditions would eventually reach their previous steady state (Fairchild & Kennedy, 2007; Kennedy and Blick, 2011). There is still debate over the mechanism that led to the formation of cap carbonates, with three models proposed by Shields (2005); deep water mixing in oceanic turn over, rapid erosion of carbonate shelves pumping more carbonate into the water, and methane gas hydrate destabilization. Cap carbonates have been found to have negative $\delta^{13}C$ values, typically around 10‰ lower than pre-glacial levels indicating changes in the global carbon cycle (Hoffman *et al.*, 1998; Fairchild and Kennedy, 2007). $^{12}C$ and $^{13}C$ are the most common stable isotopes of carbon (Hillare-Marcel and Revalo, 2007). $^{12}C$ is preferentially used in photosynthesis, leading to positive δ13C trends through most of geologic history (Hoffman, 1998). Therefore a reduction in biological productivity would lead to negative $\delta^{13}C$ values seen

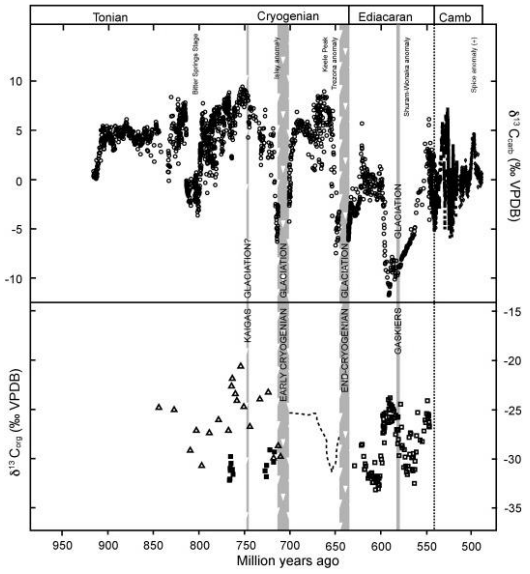


Fig.2. $\delta^{13}C$ of $C_{carb}$ and $C_{org}$ showing pre- and post-glacial negative excursions. From Halverson et al. (2010)

before the Marinoan glaciation (Halverson, 2004). The negative $\delta^{13}C$ excursion in cap carbonates is close to that of mantle values (-6‰±1) which indicates that values found in cap carbonates are likely derived from the volcanic $CO_2$ produced during a snowball Earth (Hoffman *et al*., 1998).

Banded iron formations are found primarily in the formations from the Sturtian glaciation and are seldom found in Marinoan post glacial deposits. The formation of these banded iron formations is also tied to the rapid exposure of the post glacial ocean to the atmosphere. Hypotheses for the lack of iron formations in the Marinoan have been postulated as being due to a shorter time frame, increased seafloor weathering. It has been postulated by Hoffman et al. (2017) that the formation of the Franklin large igneous province, timed prior to the onset of the Sturtian glaciation would have provided abundant iron for weathering increasing the likelihood of BIFs forming in the Sturtian glaciation.

Evidence has been found for Neoproterozoic glaciation throughout the world (Harland and Hambrey, 1982) and many of these locations have been well studied. Some of the northernmost glacial records are found on the Svalbard archipelago, where one such deposit has been well studied, while the other has received less attention from researchers.

## Geological History of Svalbard:

Svalbard is an archipelago situated approximately 1200km above the Arctic Circle. Svalbard has formations from almost every period in geologic history located within only 60.000 $km^2$ (Dallmann, 2015). The harsh tundra environment means that vegetation is sparse, and weathering of the rocks is limited, making it an ideal place to study Earth's geologic history. The oldest known rocks are those of the Southwest, Northwest and Northeast Basement Provinces (until recently known as Heckla Hoek). The oldest known rocks in the Basement Provinces have been dated to 2.7Ga, placing them in the Archean Era (Dallmann, 2015).

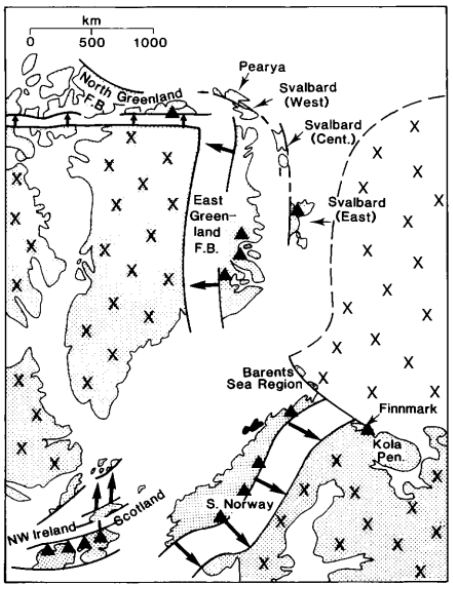


Fig. 3. Evolution of Svalbard during the Caledonian Orogeny from Fairchild and Hambrey (1994).

These rocks are primarily heavily metamorphosed meta-igneous and metasedimentary gneisses and migmatites, however among these Proterozoic rocks there are preserved sedimentary rocks from the Cryogenian. The Neoproterozoic sedimentary successions are found in the Northeastern Province and the Southwestern Province (Dallman, 2015, Harland, Hambrey and Waddams, 1993). However these two provinces were likely formed in two separate basins before being joined by strike-slip fault movement during the Caledonian Orogeny (Harland *et al*, 1993; Fairchild and Hambrey, 1994). The Northeastern Province correlate well with those

of North East Greenland (Hambrey 1983, Fairchild and Hambrey, 1995) while the Southwestern Province correlates best with the Perya terrane of Ellesmere Island, Northern Canada and with Northern Greenland (Mazur *et al*, 2011). Li et al. (2013) have compiled the earliest paleo-magnetic latitudinal determination of Svalbard's position in the Proterozoic, placing Svalbard at 26°S approximately 800Ma.


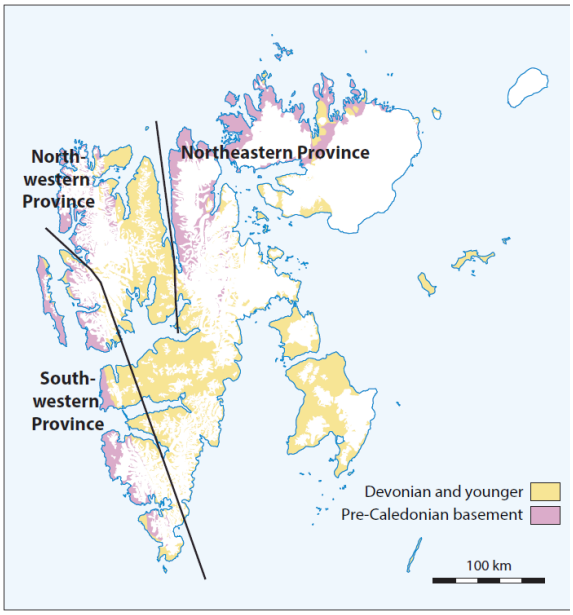


Fig. 4. (left) A map of modern Svalbard with the study site denoted by a red star.

Fig. 5. (above) the extent of Proterozoic basement rock (pink) with the geographic extent of the basement provinces marked. From Dallmann (2015).

## Important tectonic events of post-Proterozoic Svalbard:

The post Proterozoic of Svalbard was marked by several major tectonic events leading to deformation. The earliest major deformational event was the Caledonian Orogeny. It is believed at this time Svalbard was coalesced from three separate terranes through left lateral motion. This brought the Northeast and Northwest Province northwards where they joined the western province (Harland et al, 1993, Fairchild and Hambrey, 1994). Dating of granites intruding Proterozoic basement migmatites from northern Svalbard give dates of approximately 440Ma, towards the end of the Caledonian Orogeny (Dallmann, 2015).

Later deformation occurred in western Svalbard during the Eocene. As rifting occurred in the Arctic, Greenland and Svalbard moved past each other along the Hornsund Fault Complex forming the West Spitsbergen Fold and Thrust Belt (WSFTB). This motion led to compression in western Svalbard deforming the Western Basement Provinces and upturning and thrusting pre Cenozoic strata. This event deformed the Neoproterozoic sediments in the Southwest Basement Province (Bjørnerud, 1989; Kowalis and Craddock, 1984; Harland, Hambrey and Waddams, 1993).

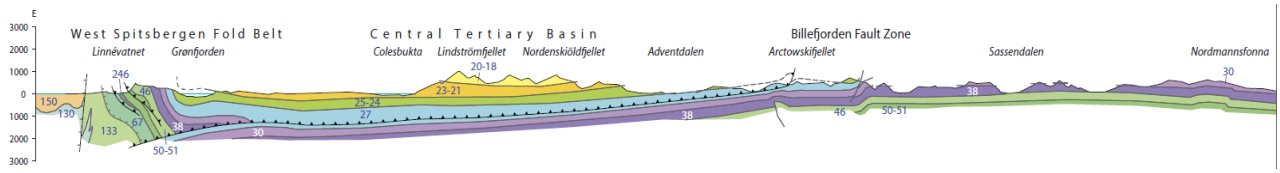


Fig. 6. Cross section of WSFTB starting from Kapp Linné (left) through Edgeøya. From Dallmann (2015).

## Neoproterozoic glacial deposits on Svalbard:

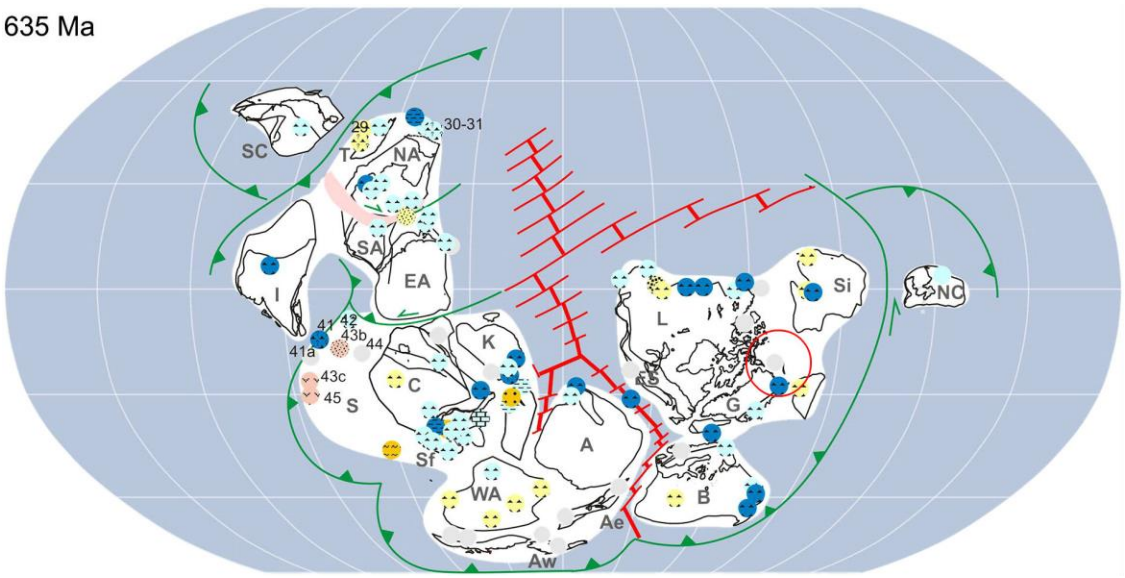


Fig. 7. Svalbard's location (red circle) at the onset of the Marinoan glaciation. Modified from Li et al (2013)

The first suggestion of a diamictite on Svalbard being glacial in origin was in a report by Garwood and Gregory (1898) which detailed their observations of a diamictite in Bellsund in the Southwestern Basement Province. Their primary investigations on Svalbard were related to glaciers and glaciogenic landforms such as eskers, moraines and till and it was apparent that the provenance of the diamictite was glacial, comparing the rock to the Reusch's Moraine in

northern Norway (Garwood and Gregory, 1898). Later work identified numerous deposits of Neoproterozoic glacial deposits throughout the Southwestern and Northeastern Basement Provinces (Harland & Wilson, 1956; Wilson and Harland, 1964, Harland, Hambrey and Waddams, 1993). The diamictites of the Northeastern Province are the most studied due to their preservation and lack of deformation (Fairchild *et al*., 2016; Harland, Hambrey and Waddams, 1993).

Fairchild and Hambrey (1984) correlated the stratigraphy in the Northeastern Province with those in East Greenland, and it has been generally accepted that these interpretations are correct, indicating that Greenland and Northeast Svalbard formed in the same basin (Halverson 2011; Halverson *et al*., 2004).

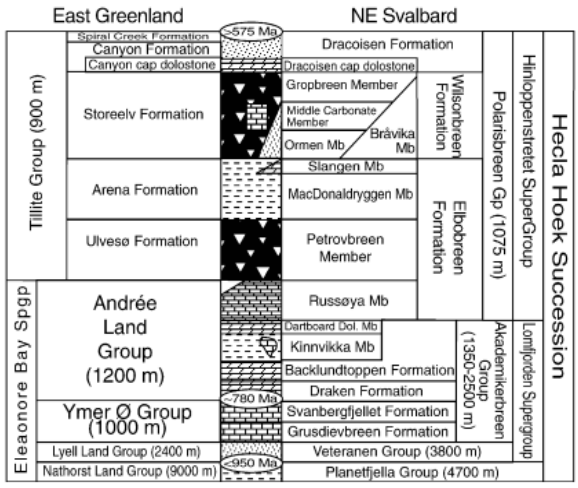


Fig. 8. Correlated Stratigraphy of East Greenland and Northeast Svalbard. From Halverson et al. (2004)

Initially it was believed that the Bellsund Group in southwest Svalbard was correlated to the Polarisbreen Group of Northeast Svalbard (Krasil'scikov 1979) though to later attempts to correlate the glacial deposits of the Southwestern Province with those of the Northeastern Province have been spurious at best (Harland, Hambrey and Waddams, 1993). Further work has shown that the differences in depositional environment preclude direct correlation and point to deposition in separate basins. (Björnerud, 2010; Fairchild *et al*., 2016).

The tillite and dolostone association in the northeast of Svalbard were noted in the Norwegian Swedish Expedition in 1931 and later investigated by later researchers. Work by Fairchild and Hambrey (1984) and Fairchild et al. (2016) and proposed a continental lacustrine depositional environment for the Polarisbreen Group based on the presence of fluvial channels and high $\delta^{18}O$ values in the cap dolostones which indicated evaporation had taken place in an arid basin while the cap dolostones were forming.

The diamictites of the Southwestern Basement Province are part of the Bellsund group found along the western coast of the island of Spitzbergen. The diamictite here several hundred meters thick, marine diamictite and is metamorphosed to greenschist facies, and contains abundant clasts of limestone and dolostone as well as limited clasts of quartzite and crystalline rocks (Kowallis and Craddock, 1984; Bjornerud 1991, 2010). Two main deformation events are believed to have affected the diamictites, the Caledonian Orogeny, and the Paleogene West Spitzbergen fold and thrust belt (Kowallis and Craddock, 1984). These tectonic events deformed the matrix of the diamictite as well as the clasts, with the least competent clasts; limestone and dolostone, showing the most deformation. The Kapp Lyell diamictite is lacking a cap carbonate

sequence south of Bellsund, however this study may have found the first cap carbonate in the sequence.

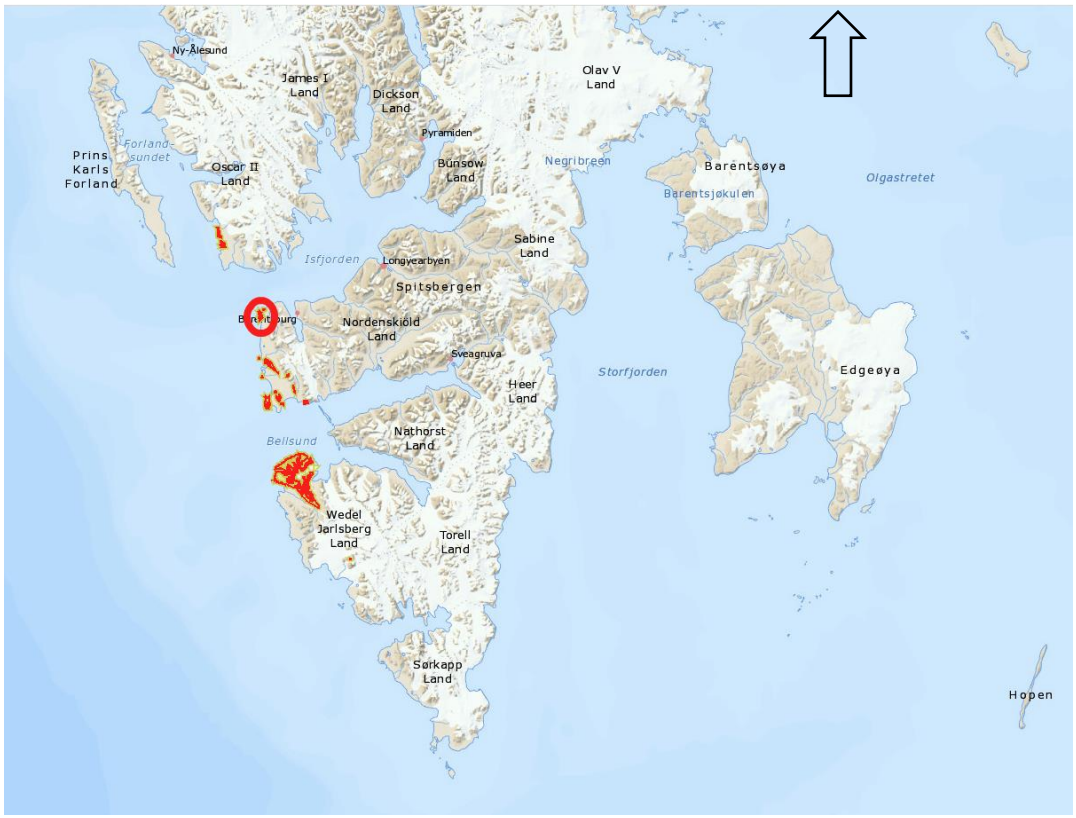


Fig.9. Map of southern Spitzbergen with the extent of the Bellsund Group in red. Circle is location of the study site.

## Aim of Study:

The aim of this study is to provide a better picture of the stratigraphy of the northern extent of the Kapp Lyell diamictites where they outcrop at Kapp Linné and to correlate the stratigraphy to that of Bellsund as well as to provide the first stable isotope analysis of the Kapp Linné sequence diamictites. Additionally, the depositional history will be interpreted to explain the formation of the Kapp Linné formation and to interpret its relevance to the Snowball Earth hypothesis and the Neoproterozoic glacial history of Svalbard.

# Methodology:

## Fieldwork

Fieldwork at Kapp Linné was carried out during two field excursions in August 2018 and March 2019. The field work in August 2018 was supported by the University Center in Svalbard, who arranged boat transportation to the study site, and in March 2019 by a local tour company that arranged a snowmobile guide to safely travel to the site.

During the fieldwork in August 2018 the site was mapped and logged. Clasts in the diamictite were counted and identified. Strike and dip measurements were taken at contacts between the various units, and their thicknesses measured where possible, and estimated where conditions were unsafe for more exacting standards. During the August fieldwork, only two samples were collected from the upper carbonate unit due to the arrival of 3 polar bears to Kapp Linné, which necessitated staying safely inside for the final day of fieldwork.

The lack of these samples necessitated the March field expedition, where samples were taken along the south facing ridge of the upper carbonate unit. Due to a recent storm the contact between the diamictite and the carbonate unit was under a thick layer of snow and ice and the start of the sample profile was located approximately 1.5m from the contact.

Fig. 10. Sample collection from carbonate unit during March 2019 fieldwork.

Samples were taken every meter. The snow was cleared, and the ice broken with a sledge hammer. The upper layer of rock was removed to approximately 10cm below the surface to remove weathered surface, and to avoid rock that has been exposed to meteoric water. At sampling location 7 through 11 the ice on the surface along the profile was too thick to break through, and for these locations sampling was done on exposed rocks approximately 1.5meters above the profile line. No sample was obtained from meter 8 along the profile due to no exposure above the ice.

## Sample preparation

All samples were cut using a rock saw at Stockholm University to provide a fresh surface. 7 of the samples were selected for polished thin sections which were prepared by Vancouver Petrographics. Thin sections were studied under a Nikon petrographic microscope and images were acquired with a Leica EC3 microscope camera attachment and a Samsung Galaxy S8 mobile phone.

All samples were analyzed using a handheld Olympus Delta X-ray Fluorescence analyzer for Ca, Fe, Mn and Mg levels and other trace elements.

## Stable isotope analysis

The carbonate samples were then micro-drilled along the fresh surface and the powder was used for analysis of $\delta^{13}C$ and $\delta^{18}O$, values as follows.

Sample KL-13A-18 and KL-09-18 were drilled at 1cm intervals to determine small scale changes in stable isotope concentration. Sample KL-10-18 was drilled at intervals of one centimeter across the fresh surface to determine if it was a concretion or a clast.

Between 230 and 270µg of each sample was collected, and dried for 24 hours at 90˚C and were then reacted with phosphoric acid overnight before analysis.

Stable isotope analysis was conducted on a GasBench III chromatograph.

The results of the tests were calibrated using standards provided by the International Atomic Energy Agency (IAEA): IAEA-CO-1 and IAEA-CO-8 as well as NBS-18. After every 10 samples, recalibration was carried out using these IAEA standards. Control samples $CaCO_3$_Merck and CARM-1 were tested to ensure accuracy of the results.

Maps were made using ArcGis and images and satellite photography used were taken from SvalbardKartet and TopoSvalbard, both produced by the Norwegian Polar Institute (NPI) and are licensed under fair use.

## Carbonate mean values

There is currently no standard for mean oxide composition of carbonate rocks. Therefore, in this paper a novel standard will be used based on a compendium of the average value of oxide weights in dolostone samples analyzed from dolostone formation from around the world: Graf (1960), Franchi (2018), Kaminskas (2010), Khalaf et al. (2018) and Lumsden (2001). Graf (1960) is a compendium of results from numerous studies, and the values used were selected at random using Wolframalpha$^{Tm}$'s random number generator. Any rock that was specifically noted to be an outlier from normal dolostone was discounted; e.g. "ironstone" or "Mn" rich. A total number of 68 samples were used to create this mean. The results of this average are presented in the following table:

| Oxide | Average % |
|---|---|
| SiO2 | 9,12 |
| Al2O3 | 1,07 |
| Fe2O3 | 0,97 |
| MnO | 0,18 |
| MgO | 20,59 |
| CaO | 29,61 |
| K2O | 0,21 |

From here this will be referred to as the Mean Dolostone Value (MDV).

# Results:


Fig.11. Satellite image of Kapp Linné with the extent of the area studied in August 2018 in green. Image from NPI.

## Study Area Description:

Kapp Linné is situated on the central western coast of Svalbard at the entrance to Isfjord. A former radio station, now a hotel makes this an ideal area for study with regards to safety considerations. The geologic units are inferred to be from the Neoproterozoic due to their lack of fossils(Harland, Hambrey and Waddams, 1993). Prior work at Kapp Linné has described the Kapp Linné formation as a diamictite with some marbles and phyllite (Harland, Hambrey and Waddams, 1993; Hjelle, 1962) though no detailed investigation of the area has been conducted. To the west of the lake Frysjoen there is an outcrop of grey quartzite representing the lowest unit in the sequence (Harland, Hambrey and Waddams, 1993). Kapp Linné and the surrounding area was submerged under water as recently as 10,000 years ago, rising above the surface as post-glacial rebound raised the land after the melting of the ice sheets of the Weichselian glaciation, giving the area a thicker sediment cover than most of Svalbard (Forman and Ingólfsson, 2001).

Fig. 12. The Kapp Linné sequence looking east with the general eastward dipping trend. Note the tension gashes in the carbonate unit on the right side of the image.

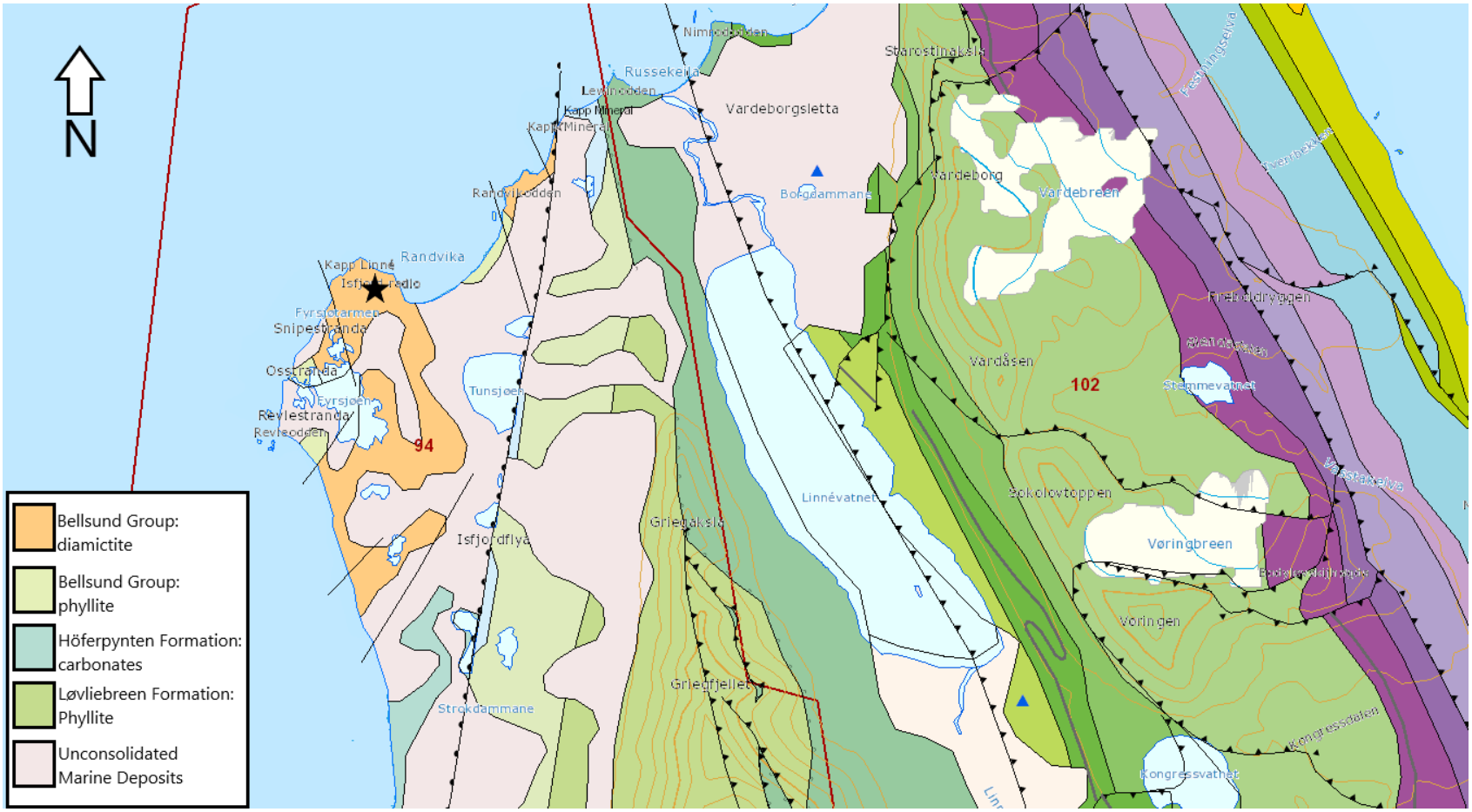


Fig. 13. A geologic map showing Kapp Linné (marked with a star) and the surrounding areas. Note the upturned strata of the Mesozoic to the east, upturned by the WSFTB. Image and data taken from SvalbardKartet, NPI.

## Stratigraphy:

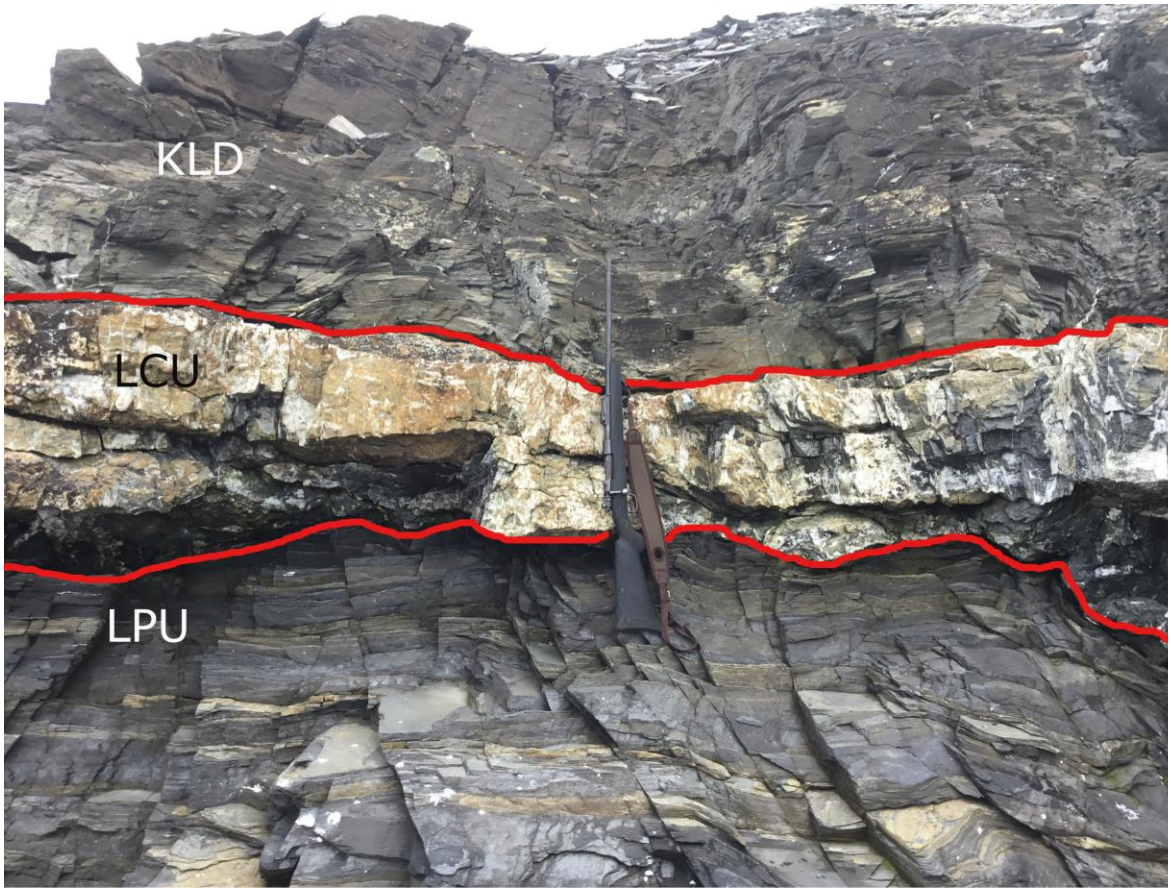


Fig. 14. Stratigraphy of the western side of the study area. KLD is the Kapp Linné diamictite. LCU is lower carbonate unit LPU is the lower phyllite unit. The rifle is approximately 1.5m in length.

The Kapp Linné diamictite (KLD) is a green to red weathering diamictite that has been metamorphosed to greenschist facies. The primary clasts contained in the KLD are limestone and dolostones, with occasional granites and quartzites. The clasts have been deformed on the parallel to the metamorphic foliation, with the less competent limestone clasts often flattened and boudinaged. Less deformation is seen in the dolostone, and almost no deformation seen in the granite or quartzite clasts. Preserved clast lenses are found oriented parallel to the lamination (see fig. 13/14).

The KLD dips gradually to the east the western part of the study site, and dips near vertically in the east approaching Randvika. Larger stones are more abundant in the upper part of the unit. Where the diamictite is in contact with the lower units finely bedded lamination is seen (Fig.14) and becomes massively bedded higher in the bed, and towards the south of the study area. Two thin sections were made from the KLD to determine the component minerals and metamorphic grade (Fig. 15,16) Abbreviations for minerals seen in thin section taken are from Whitney and Evans (2010).


Fig. 15. The Kapp Linné Diamictite. (A) Finely bedded laminated diamictite from the eastern section. Note the clast lens in the center. (B) Massively bedded diamictite in the southern section. (C) Clast rich diamictite

Fig. 16. Detail of preserved mud lens from the KLD. Scale on the ruler is in millimeters.

Fig. 17. Clast lens from Fig. 13 in situ.

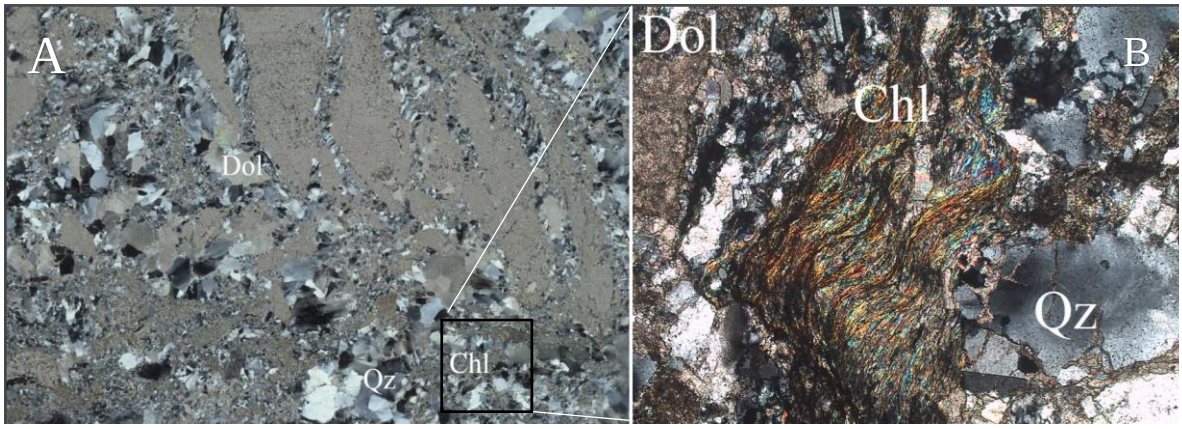


Fig. 18. Thin section of KLD in XPL of sample IFR-02-19. (A) The Dol clast shows micritic texture. Secondary Qz and recrystallized dolomite are seen, with minor Chl present in the diamictite. (B) Thin section at 20X magnification showing undulating Qz indicating strain from tectonic forces.

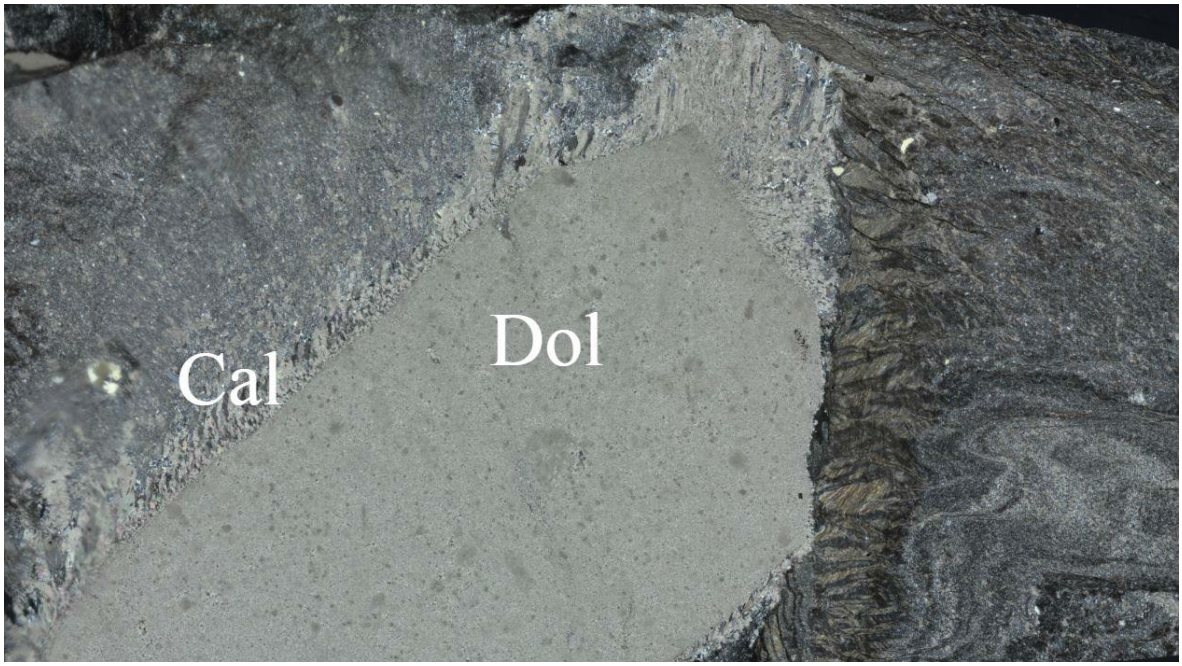


Fig. 19. Thin section scan in XPL of Dol clast in the diamictite. Infill can be seen above and to the left of the clast indicating volume loss during metamorphism. The curved calcite to the left indicates rotation in

Fig. 20. Fresh surface of the lowest section of the KLD showing alternating grain size. White is the course, grey fine bedding. Way up is to the right

The KLD sharply overlies the Lower Carbonate Unit (LCU), an orange to cream weathering dolomite layer averaging .5-1m thick in the west of Kapp Linné. The lowest section of this unit is finely laminated and marly, while the upper part of the unit is massive with no bedding/foliation.


Fig.21. (A) (B) Contact between the KLD and the LCU in the western section.

(C) Fine laminations at the base of the KLD


Fig. 22. Details of the LCU in the western section of Kapp Linné. (A) Apparent draping over a large carbonate body. (Rifle is 1.5m) (B) Close detail of LCU where samples KL-13A/13B-18 were taken. (C) Abrupt truncation of the LCU. West is to the right in the image. (D) Detail of possible draping over the large carbonate mound seen in (A).

The LCU has secondary quartz and calcite veining. The upper part of the unit contains abundant pyrite, both euhedral and framboidal. Minor pyrite was observed in the lower part of the LCU. The LCU is discontinuous, found in the eastern section and abruptly truncated to the west of the locality shown in Fig. 11 (see Fig. 14.C). The LCU in eastern Kapp Linné dips southwest and grades upwards into a calc-shale that is approximately 10m thick.

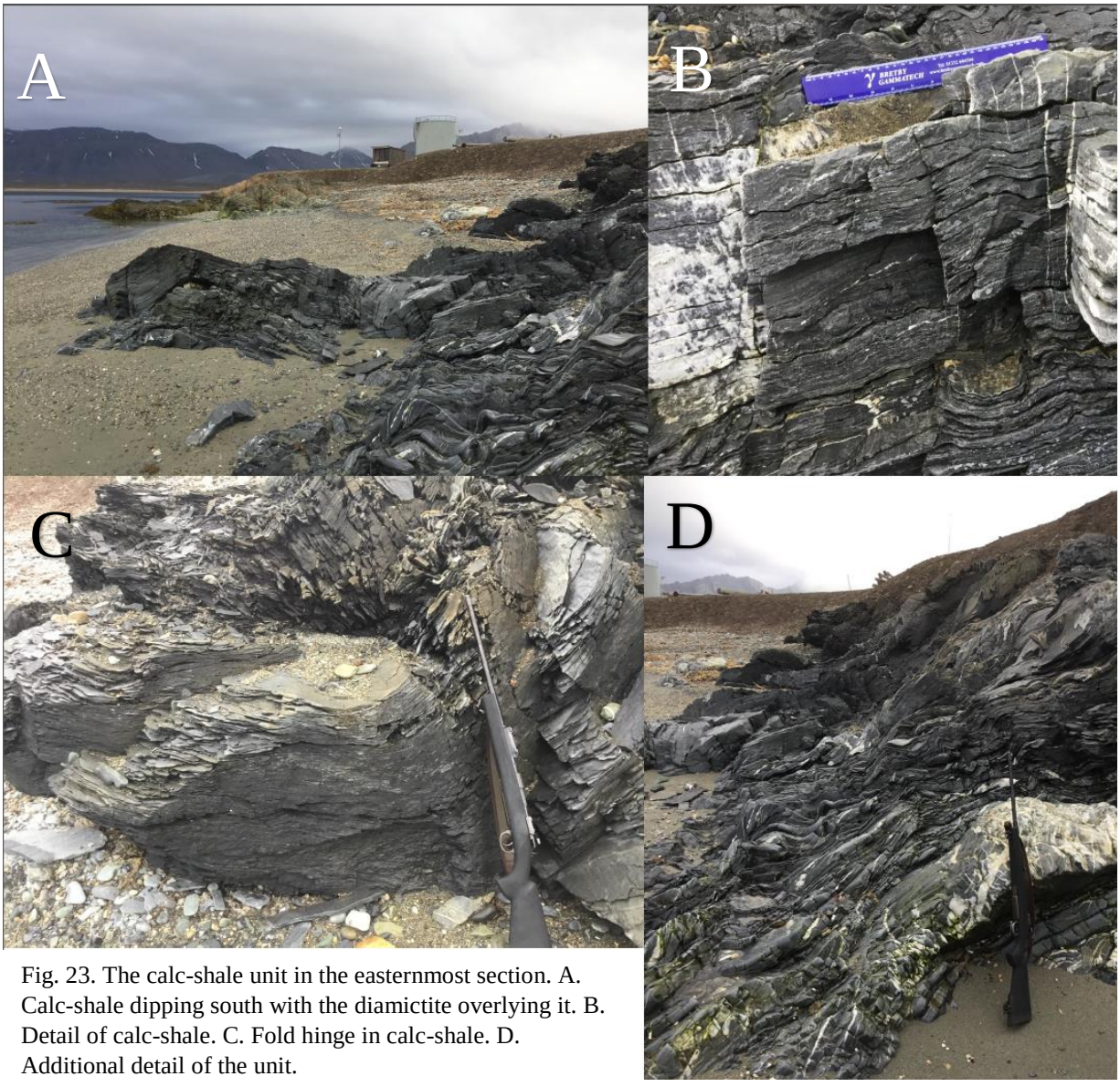


Fig. 23. The calc-shale unit in the easternmost section. A. Calc-shale dipping south with the diamictite overlying it. B. Detail of calc-shale. C. Fold hinge in calc-shale. D. Additional detail of the unit.

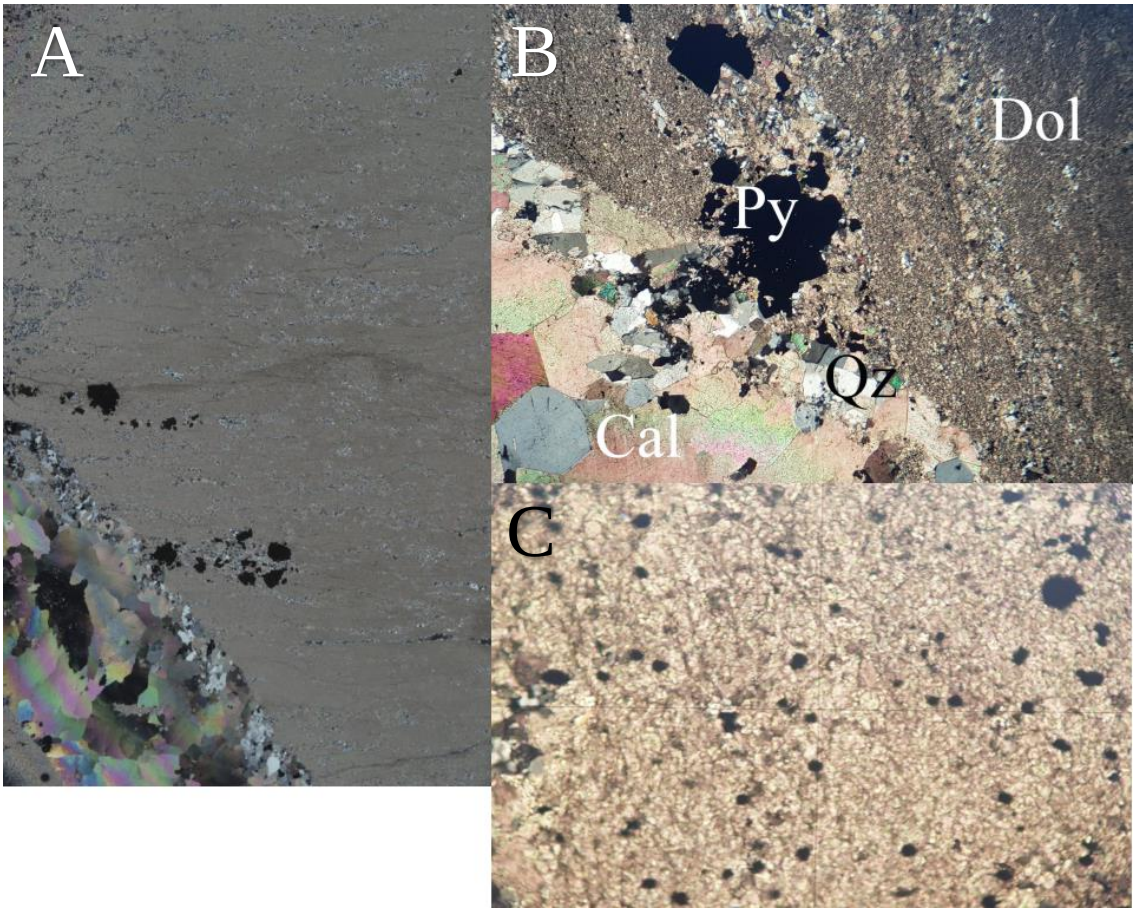


Fig. 24. (A)This thin section from the LCU shows a micrite texture with a calcite vein in the bottom left. Euhedral pyrite is seen in the lower center and center left. (B)KL-13A at 20X magnification under XPL showing the Qz boundary at between the Cal vein and the Dol. The opaque minerals are euhedral Py. (C) Framboidal Py at 20X in transmitted light.

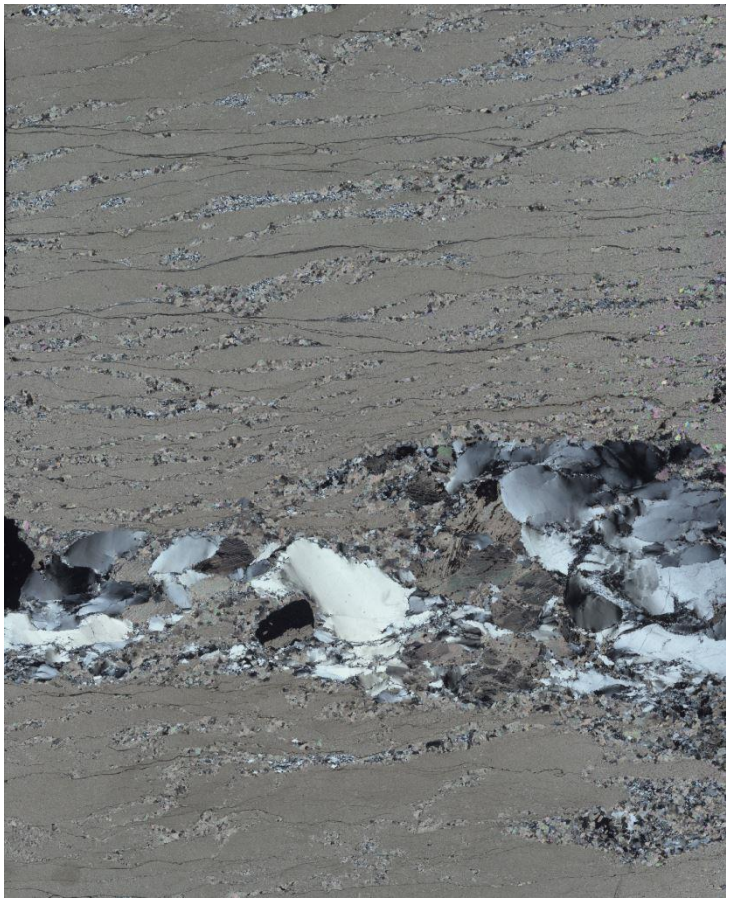

Fig. 25. Thin section from the calc-shale section of the LCU. Note the fine dark layers which contain white mica, and are may be formed along the original lamination.

The lower phyllite unit (LPU) is situated unconformably below the LCU with an erosional contact. The LPU contains some sandy lenses that have been metamorphosed to quartzite nearing the contact with the LCU. The lowest section observed at Kapp Linné was a sandy carbonate unit (SCU) situated under the LPU. Due to poor conditions during the March 2019 fieldwork no photos were obtained of the SCU.

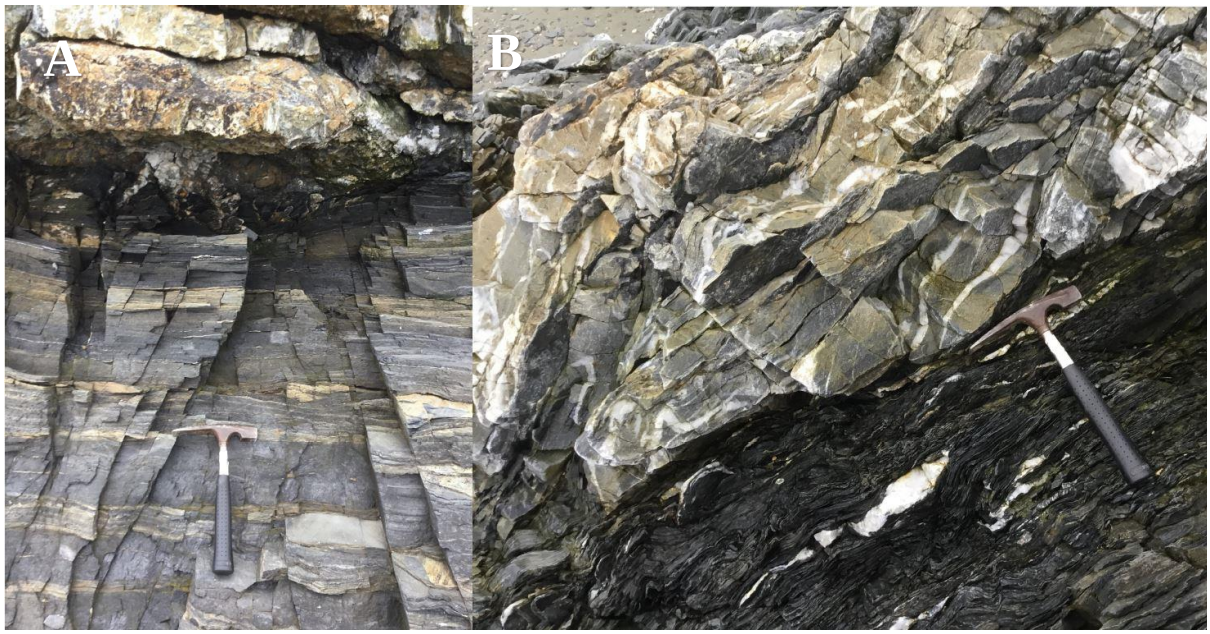


Fig. 26. The contact between the LCU and the LPU in the west (A) and the east (B) of Kapp Linné. In (A) the quartzite is seen in the beige lenses. The dip here was 24°E. (B) The eastern outcrop of the LPU is dipping almost vertically. The image is taken facing straight down. Hammer is approximately 20cm.


Fig. 27. Hand sample of the sandy carbonate unit.

At the eastern section of the study area located near the hotel at Kapp Linné there is a vertically dipping diamictite apparently underlying a carbonate unit, though sediment cover and inability to investigate the stratigraphy along the shore makes the position in the stratigraphy difficult to determine. This upper carbonate unit (UCU) appears to overlay the KLD in the center the syncline. The dip of the diamictite at the contact was measured to be 78˚ towards the west. The upper carbonate unit is a pink-grey weathering diamictite with abundant secondary quartz veining. The unit lacks the pyrite as well as the lamination/foliation of the LCU.

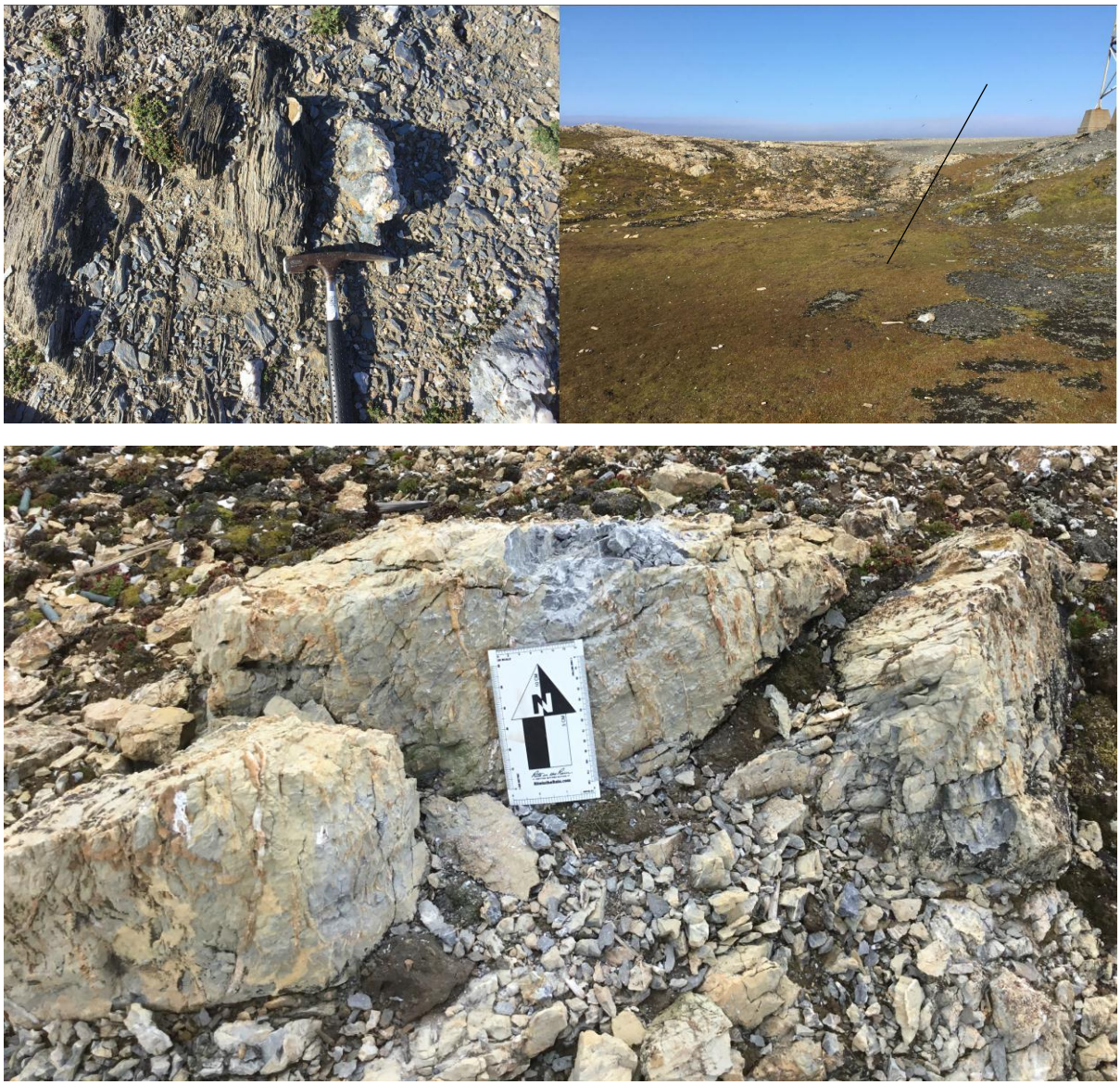

Fig. 28. The contact between the KLD right and the UCU (left) The UCU (left) at the contact with the KLD denoted by black line. (Lower) Outcrop of the UCU with fresh surface exposed.

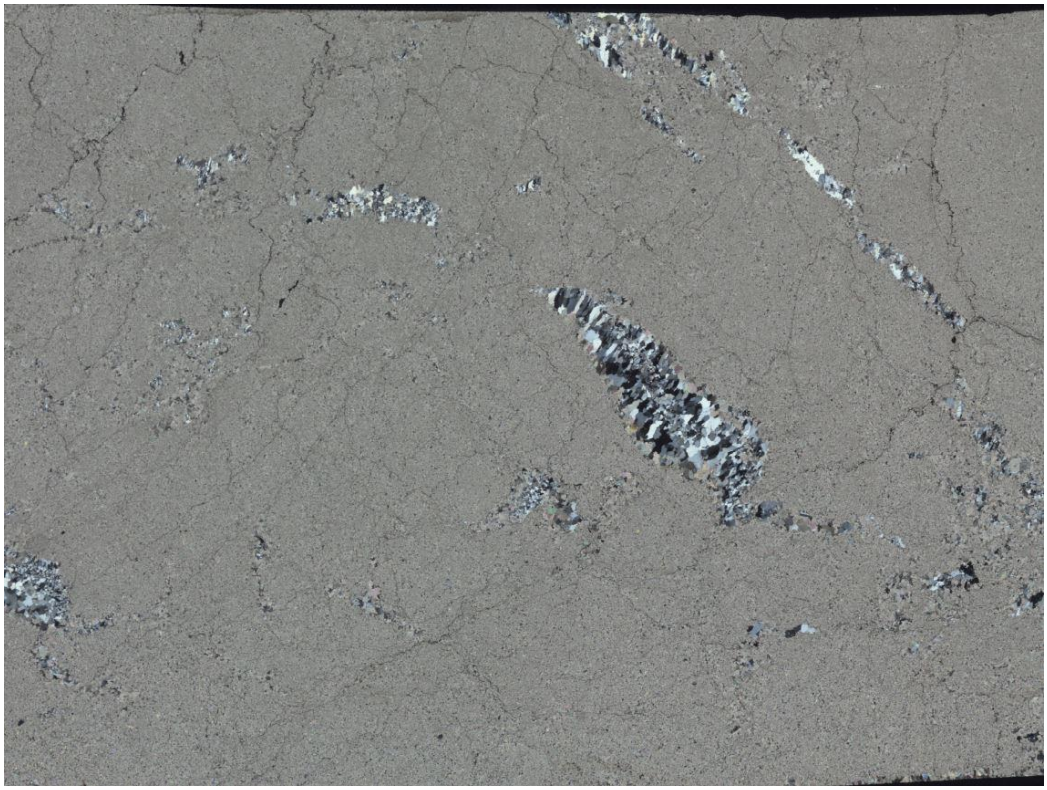

Fig. 29. Thin section from the upper carbonate unit showing micritic dolostone and secondary quartz.

## Isotope and Oxide Analysis:

Table 1. List of analyzed samples.

| Sample ID | Sample Description |
|---|---|
| IFR-04-19 | Sandy carbonate unit |
| KL-14-18 | Lower phyllite unit |
| KL-13B-18 | Lower part of the lower carbonate unit |
| KL-13A-18 | Upper part of the lower carbonate unit |
| KL-15-18 | Eastern LCU shale |
| KL-12-18 | Diamictite |
| KL-10-18 | Dolostone clast from diamictite |
| IFR-02-19 | Diamictite |
| IFR-03-19 | Diamictite with quartz intrusion |
| IFRCC-01-13-19 | Upper Carbonate Unit |

## XRF Results:

Table 2.

XRF results 2018 samples:

| | KL-13A-18 | KL-13B-18 | KL-02-18 | KL-14-18 | KL-15-18 | KL-10-18 | KL-12-18 |
|---|---|---|---|---|---|---|---|
| CaO | 28.37 | 31.17 | 19.26 | 1.44 | 29.22 | 33.68 | 6.56 |
| $SiO_2$ | 21.34 | 7.48 | 13.94 | 45.86 | 19.64 | 0 | 77.65 |
| $Fe_2O_3$ | 5.27 | 4.34 | 2.34 | 7.57 | 3.84 | 0 | 6.67 |
| $Al_2O_3$ | 0 | 0 | 0 | 15.43 | 0 | 0 | 15.47 |
| MnO | 0.35 | 0.65 | 0.28 | .042 | .60 | .0185 | .088 |
| LE | 64.18 | 70.57 | 70.3 | 58.21 | 65.99 | 75.7 | 42.99 |

Except for the LPU and the diamictite the samples are primarily carbonate with minor Si and Fe. The LPU and KLD show the greatest variance in their composition with lower Ca and K, Al and Si dominating the non LE.XRF Results for Upper Carbonate Unit samples:

Table 3. UCU XRF results.

| | KL-09-18 | IFRCC-01-19 | IFRCC-02-19 | IFRCC-03-19 | IFRCC-04-19 | IFRCC-05-19 | IFRCC-06-19 | IFRCC-07-19 | IFRCC-09-19 | IFRCC-10-19 | IFRCC-11-19 | IFRCC-12-19 | IFRCC-13-19 | IFRCC-16-19 |
|---|---|---|---|---|---|---|---|---|---|---|---|---|---|---|
| $SiO_2$ | 7.46 | 8.06 | 7.27 | 9.58 | 14.53 | 8.83 | 14.78 | 8.56 | 8.36 | 7.383 | 17.59 | 14.57 | 9.39 | 11.19 |
| CaO | 31.1 | 30.03 | 30.50 | 29.89 | 28.7 | 32.36 | 30.38 | 32.27 | 30.88 | 31.22 | 28.21 | 28.33 | 30.82 | 34.07 |
| $Fe_2O_3$ | 4.34 | 3.03 | 2.55 | 3.27 | 3.01 | 3.60 | 3.77 | 4.26 | 2.58 | 2.67 | 2.84 | 3.23 | 2.67 | 3.54 |
| MnO | 0.33 | 0.24 | 0.20 | 0.29 | 0.24 | 0.33 | 0.30 | 0.32 | 0.28 | 0.29 | 0.29 | 0.27 | 0.29 | 0.33 |
| LE | 25.41 | 26.54 | 29.28 | 25.59 | 21.74 | 21.95 | 16.59 | 21.82 | 26.66 | 28.69 | 18.29 | 21.65 | 26.26 | 13.89 |

The UCU samples are dominated by CaO with varying levels of Fe. Cl was present in 60% of the samples likely due to their proximity to the sea and as such is disregarded in this study.

## Stable Isotope Results.

From lowest unit to uppermost unit. The error range for stable isotope values as measured on the Stockholm University Gasbench II are ±0.07‰ for $\delta^{13}C$ and ±0.15‰ for $\delta^{18}O$.

Table 4:
IFR-04-19

| $\delta^{13}C$ | $\delta^{18}O$ | %VSMOW |
|---|---|---|
| 4.48 | -10.57 | 20.02 |

The limestone unit shows positive δ13C values and negative δ18O values.

Table 5:
KL-13B-18

| $\delta^{13}C$ | $\delta^{18}O$ | %VSMOW |
|---|---|---|
| -3.30 | -11.52 | 19.05 |

Table 6:
KL-13A-18

| | δ13C | δ18O | %VSMOW |
|---|---|---|---|
| Cm 1 | -3.11 | -11.60 | 18.97 |
| Cm 2 | -3.03 | -12.15 | 18.39 |
| Cm 3 | -3.04 | -13.50 | 17.00 |
| Cm 4 | -3.00 | -11.76 | 18.79 |
| Cm 5 | -2.93 | -12.57 | 17.97 |
| Cm 6 | -3.00 | -11.94 | 18.61 |
| Cm 7 | -2.92 | -11.58 | 18.99 |
| Cm 8 | -3.00 | -11.80 | 18.75 |

The lower carbonate unit shows a consistent negative $\delta^{13}C$ values and negative $\delta^{18}O$ values

Table 7:
KL-15-18

| $\delta^{13}C$ | $\delta^{18}O$ | %VSMOW |
|---|---|---|
| -3.29 | -11.63 | 18.93 |

The calc-shale above the LCU shows similar stable isotope values to the western section of the LCU.

Table 8:
KL-12-18

| | $\delta^{13}C$ | $\delta^{18}O$ | %VSMOW |
|---|---|---|---|
| A | -0.97 | -13.50 | 17.00 |
| B | -1.86 | -18.21 | 12.15 |

The diamictite shows higher $\delta^{13}C$ values than the lower units along with the most negative of the $\delta^{18}O$ values seen at Kapp Linné.

Table 9:
KL-09-18

| | $\delta^{13}C$ | $\delta^{18}O$ | %VSMOW |
|---|---|---|---|
| Cm 1 | -2.92 | -11.25 | 19.32 |
| Cm 2 | -2.47 | -11.46 | 19.10 |
| Cm 3 | -2.55 | -12.07 | 18.47 |
| Cm 4 | -2.08 | -12.56 | 17.97 |

This sample was taken at the contact with the KLD

Table 10:
IFRCC-19

| $\delta^{13}C$ | $\delta^{18}O$ | %VSMOW |
|---|---|---|
| -2.62 | -11.65 | 18.91 |
| -2.53 | -11.53 | 19.03 |
| -2.37 | -12.29 | 18.25 |
| -3.01 | -11.05 | 19.53 |
| -2.81 | -11.57 | 19.00 |
| -2.52 | -12.63 | 17.90 |
| -2.81 | -11.92 | 18.64 |
| -3.01 | -11.09 | 19.49 |
| -2.81 | -10.56 | 20.04 |
| -2.85 | -10.07 | 20.54 |
| -2.38 | -12.54 | 17.99 |
| -2.77 | -11.78 | 18.78 |

The “cap carbonate” series shows relatively stable trends throughout the unit, with -$\delta^{13}C$ values as well as negative $\delta^{18}O$ values. The values are approximately -0.5‰ lower than the values of the lower carbonate unit.

Table 11:
KL-10-18

| | $\delta^{13}C$ | $\delta^{18}O$ | %VSMOW |
|---|---|---|---|
| Cm 1 | 5.03 | -4.37 | 26.42 |
| Cm 2 | 4.81 | -3.73 | 27.08 |
| Cm 3 | 5.31 | -2.01 | 28.84 |
| Cm 4 | 4.99 | -3.19 | 27.63 |
| Cm 5 | 5.00 | -4.14 | 26.65 |
| Cm 6 | 5.23 | -1.76 | 29.10 |
| Cm 7 | 5.09 | -2.54 | 28.30 |
| Cm 8 | 4.76 | -2.19 | 28.67 |
| Cm 9 | 4.95 | -2.46 | 28.39 |
| Cm 10 | 4.68 | -2.48 | 28.36 |

The clast taken from the KLD was measured across the profile to determine if it was deposited or if it grew in situ. Positive $\delta^{13}C$ values were seen in the clast, with the higher $\delta^{18}O$ values compared to the rest of the stratigraphy.

Figure 24: shows the stable isotope values and oxide percentage plotted along the stratigraphy. With the exception of the SLU and the dolostone clast, the stratigraphy shows negative $\delta^{13}C$ trends, with the values increasing in the KLD, and decreasing the UCU.

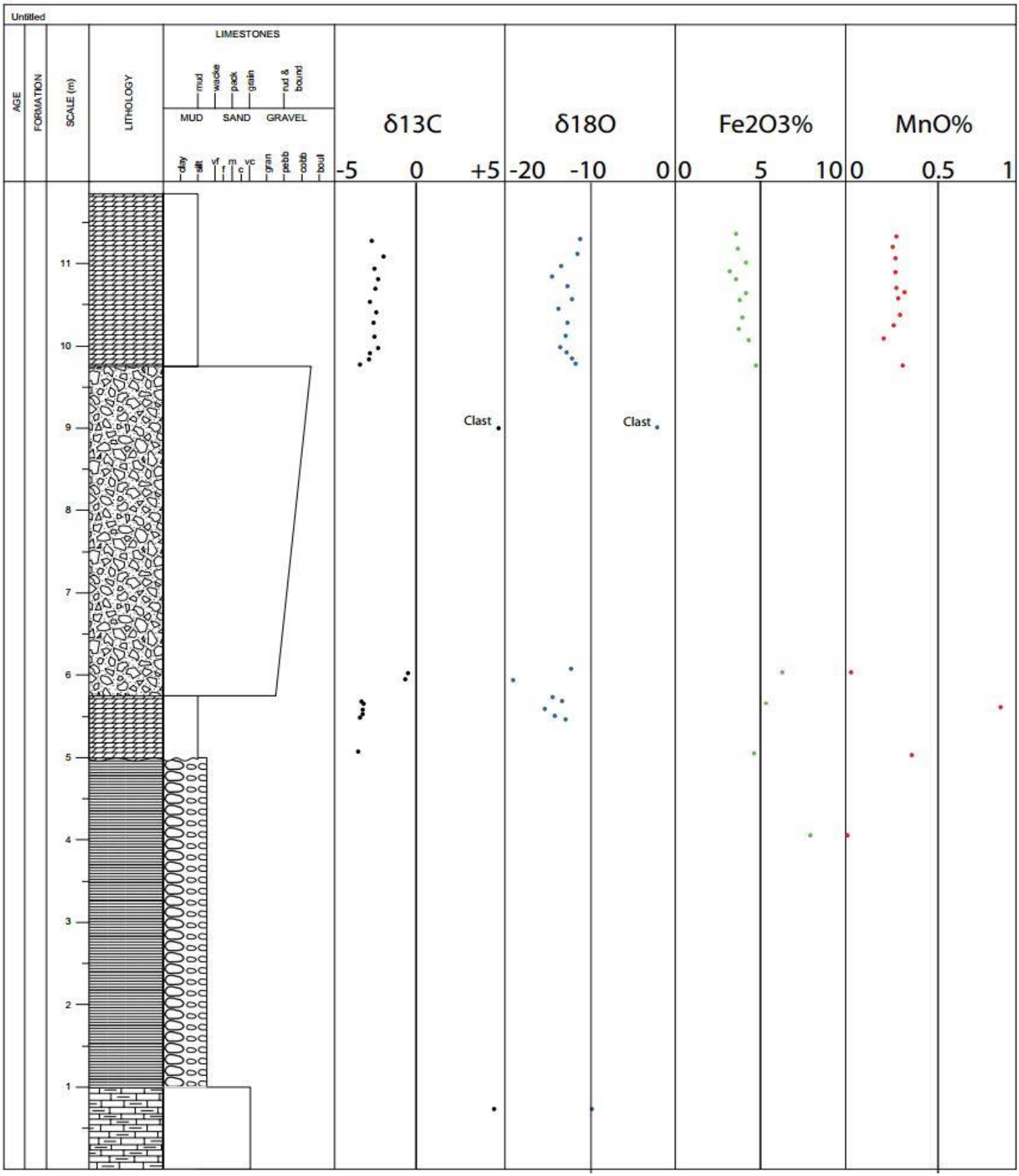


Fig. 30. A plot of the stable isotope values against the stratigraphy of Kapp Linné. $\delta^{13}C$ and $\delta^{18}O$ standard deviation are 0.07‰ and 0.15‰ respectively. FeO standard deviation values are approximately ±.02% and Mn ± 90%

# Discussion

## Chemostratigraphy at Kapp Linné:

### Stable Isotopes

The lowest stratigraphic unit at the site, the SCU unit was the only section of the stratigraphy to show a positive $\delta^{13}C$ value. Higher in the stratigraphy the LCU shows a negative $\delta^{13}C$, roughly -3‰ below the diamictite, while the dolomite in the diamictite has a $\delta^{13}C$ of -1.87‰ and -0.97‰. The UCU shows a similar negative $\delta^{13}C$ excursion than the lower carbonate unit, between -2.08 and -3.01‰ throughout the samples tested. $\delta^{13}C$ is an ideal standard to use as carbon is less likely to be affected during metamorphism. (Ferry, 1987).

The key identifier of a "snowball Earth" sequence is the presence of a cap carbonate layer of microcrystalline dolomite immediately above a diamictite that show a negative $\delta^{13}C$ excursion and increased Fe and Mn values (Hoffman, 1998; 2017). The change from a positive $\delta^{13}C$ to a negative $\delta^{13}C$ between the SCU and the LCU indicates that a change in the carbon cycle that is likely related to the cooling of the Earth and changes to the carbon cycle during the initiation of a snowball Earth. Negative $\delta^{13}C$ values in carbonates underlying glacial sediments are found beneath the Petrovbreen Member diamictite in the northeastern Svalbard Cryogenian deposits with values as low as -7‰ measured (Halverson, 2004). Further studies have found that this pre Marinoan $\delta^{13}C$ anomaly occurred concurrently globally, with negative $\delta^{13}C$ values found in China (Xiao *et al*., 2008), Namibia (Halverson *et al.*, 2002) Australia (Rose *et al.*, 2012). While the pre-glacial negative $\delta^{13}C$ excursion found at Kapp Linné is not as extreme as these other excursions, it adds further evidence to a change of the carbon cycle occurring on a global scale before the Marinoan glaciation.

The $\delta^{18}O$ values of all rocks measured showed high levels of $^{16}O$ through the stratigraphy. The $\delta^{18}O$ at Kapp Linné is the lowest in the dolomite in the diamictite at the base of the KLD, which may indicate that some of the carbonate in the matrix the rock was precipitated from $^{16}O$ enriched glacial meltwater similar to the Petrovbreen member. (Fairchild *et al.*, 2016). The values for $\delta^{18}O$ are typical of Neoproterozoic glacial deposits.

### Oxides

In the Marinoan cap carbonates BIFs are rare, though elevated iron levels can be found (Hoffman *et al*., 2017). The FeO values in the UCU range from 3-6% which places the Fe content well above the MDV suggesting that this unit formed after precipitation of iron after a buildup in anoxic conditions in a post-snowball Earth environment. Recent work on snowball Earth deposits in China report similar values of iron oxides at the base of a Sturtian cap carbonate in to those found at Kapp Linné (Feng *et al*,. 2016). Mn values in the carbonate significantly higher than the MDV of .04% by weight with the highest measured value being 0.65% by weight (5050ppm) in the LCU. Significantly lower Mn values are found in the LPU, the KLD as well as in the single carbonate clast sampled from the KLD. The KLD had the highest Mn value of the non-carbonate at 0.088% by weight (317ppm) indicating that Mn values were not affected by diagenetic processes or metamorphic fluids.

When compared to a selection of Mn and Fe oxide values from cap carbonates from both the Marinoan and Sturtian glaciations, the values of the dolostone at Kapp Linné are more similar to those of Sturtian age.

Table 12:

A comparison of major oxides in cap carbonates to the MDV.

| | MDV | Mean Kapp Linné values | Meyer et al. (2012) mean values(Sturtian, Idaho) | Feng et al. (2016) mean values (Sturtian, China) | Font et al. (2006) mean values (Marinoan, Brazil) | James et al. (2001) mean values (Marinoan, Canada) |
|---|---|---|---|---|---|---|
| SiO2 | 9,12 | 11.56 | 3.6 | 3.78 | .62 | -- |
| Fe2O3 | 0,97 | 3.46 | 2.38 | 6.03 | .45 | 1.136 |
| MnO | 0,18 | 0.32 | .68 | .41 | .18 | ,07 |
| CaO | 29,61 | 30.46 | 22.4 | 29.26 | 31.6 | 20,62 |

## The depositional environment of the KLD:

The depositional environment of the KLD is difficult to ascertain due to the deformation and metamorphism of the rock. The lowest section of the KLD shows millimeter scale turbidity layers at the base with fining upwards sequences that can be seen in Fig. 15 and 18c, which point to variations in the deposition rate. These structures have been observed in the Kapp Lyell diamictite sequences found south of Bellsund, and were interpreted as laminations (Cowallis and Kraddock, 1984; Birkenmeijer, 2003, 2010; Bjørnerud 2010) Similar varved structures are found at the base of glaciers trapped in place by year-round sea ice known as a sikussak. (Dowdeswell *et al*., 2008) Bjørnerud (2010) proposed that these laminations in the KLD formed in a similar way, however the laminated sediments at Kapp Lyell are over 1000m thick, while at Kapp Linné they are only 2-3m thick throughout the sequence, potentially pointing to a different depositional regime or distance from the glacial margin. Higher in the KLD larger clasts are found and these tend oriented parallel to the bedding/foliation. Less competent clasts such as limestone are boudinaged, and almost “smeared” in the along the foliation direction. Dolomite clasts are more competent and show some deformation and flattening with asymmetrical tails, an indication of bedding parallel shear (Bjørnerud, 1991) (see Fig. 31) while the quartzite and granite clasts are rotated. The large clasts above the laminated diamictite appear

Fig. 31. A granite clast situated above a dolostone clast. The granite clast has been rotated, and the dolostone clast has been rotated and elongated.

to deform the bedding much like dropstones. Prior work on the Kapp Lyell diamictites (Cowallis and Kraddock, 1984; Harland, Hambrey and Waddams, 1993, Bjørnerud, 1989, 2010) have identified these as dropstones, and the observations made at Kapp Linné seem to support this based on the elongated dolostone clasts having asymmetric tails (see Fig. 26 and 12.c) and apparent fining upwards sequence in the lower KLD.

### Correlation of the KLD to the Bellsund Group:

The KLD and the Kapp Lyell diamictites can be correlated based on their similar structures and the isotope analysis of clasts. Bjørnerud (2010) conducted stable isotope analysis from dolomite clasts from the Kapp Lyell diamictites and compared these values to the stable isotopes from the dolomite of the Sletfjelldalen formation in the vicinity of Bellsund and Kapp Lyell. $\delta\ ^{13}C$ and $\delta^{18}O$ in the lower Sletfjelldalen formation were +5.8‰ and -10.85‰ similar to the values of the clast tested from Kapp Linné (see table 11) respectively which are similar values to the single dolostone clast sampled from the KLD pointing to the clast originating from the underlying layers. It should be noted that only one clast was analyzed for this study, and three in Bjørnerud (2010) which gives a limited data set, but it provides a base for correlation.

Prior work in Bellsund (Kowallis and Craddock, 1984; Bjørnerud, 1989, 2010) determined the laminated diamictite at the base of the Kapp Lyell sequence to be approximately 1000m thick, while at Kapp Linné the laminated section of the diamictite is approximately 5-10 m thick before becoming massively bedded. There is a distinct lack of intervals of carbonate units in the Kapp Lyell sequence as observed by prior studies (Kowallis and Craddock, 1984; Harland, Hambrey and Waddams, 1993; Bjørnerud 1989, 2010) which points to the possibility of a different depositional environment, likely more proximal to the glacial marine margin compared to that of the Kapp Lyell formation.

Based on this study the suggested correlation of the stratigraphy at Kapp Lyell (Kowallis and Craddock, 1984) and Kapp Linné is seen in Fig. 27. The diamictites and the phyllites are the easiest to correlate. The thin limestone unit at the base of the may correlate to the SCU, however there is no lithology provided beyond what is presented in the stratigraphic log presented.

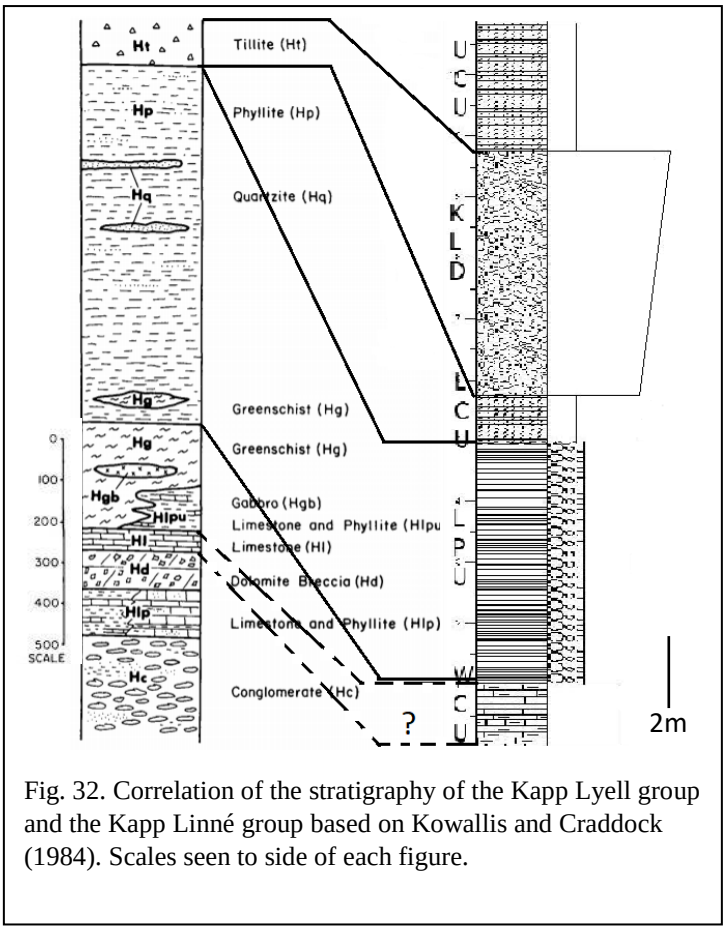


Fig. 32. Correlation of the stratigraphy of the Kapp Lyell group and the Kapp Linné group based on Kowallis and Craddock (1984). Scales seen to side of each figure.

The difference in thickness between the Kapp Linné and Kapp Lyell stratigraphy is unlikely to be due to shearing or tectonic shortening as both rocks show similar levels of metamorphism and shearing (Kowallis and Craddock, 1984; Bjørnerud, 1989, 1991, 2010; Harland, Hambrey and Waddams, 1993), indicating differences sediment input. It is likely that the southern portion of the Bellsund group was deposited in a deep basin, as evidenced by the thickness and observation of potential mass flow structures (Kowallis and Craddock, 1984; Birkenmeijer, 2003). The presence of thin carbonate layers beneath the deep marine deposits south of Bellsund (Fig. 27) may point to syn-depositional rifting similar to a suggestion by Ali et al. (in press) regarding lateral thickness variations in the Garvellachs Cryogenian formation of Scotland.

## Correlation with the Polarisbreen Group

Correlation of the Kapp Linné series with the Cryogenian deposits of the Polarisbreen formation of northeast Svalbard is not likely. While similar stable isotope values are found, work by Fairchild *et al*. (2016) interprets the Neoproterozoic glacial sequence of the northeast Svalbard to be continental in origin, comparing it to the McMurdo Dry Valleys of Antarctica. The presence of apparent dropstones, and the underlying LPU sediments point to an outer shelf to deep marine depositional environment for the Kapp Lyell group. Additionally the three terrane model of Svalbard points to the formation of Svalbard through suturing during left lateral transpression during the Caledonian orogeny (Fairchild and Hambrey, 1995; Mazur *et al*., 2011).

## A pre-diamictite cap carbonate?

The geochemistry of the LCU presents a challenge in interpreting the stratigraphy at Kapp Linné. A carbonate unit below the diamictite with a negative $\delta^{13}C$ values is not uncommon in carbonates beneath Marinoan glacial deposits. $\delta^{13}C$ values ranging from -7‰ to -11‰ have been found on Svalbard (Halverson *et al*.,2004) China(cite) Namibia (Halverson *et al.*, 2002) and Australia (Walter *et al*., 2004). The LCU however shows distinct similarities to a cap carbonate, despite underlying a diamictite. It is composed of micritic dolomite (Shields, 2005) that is possibly laminated, (though the foliation makes direct determination difficult), abundant framboidal pyrite (Jiang et al, 2003; Giddings and Wallace, 2009) and negative $\delta^{13}C$ values. High MnO values of up to .65% (see tables 2 and 3) by weight were recorded from XRF analysis of the base of the LCU. This combined with FeO values of up to 4.7% by weight points to deposition after an anoxic event with hydrothermally produced Fe and Mn building up in the water until the sea ice cover melted, the hypothesis presented for the presence of high levels of Fe and Mn in cap carbonates from snowball Earth sequences.

This raises the question of how a "cap" carbonate can form before the deposition of glacial sediments. The KLD shows fine lamination at the base, with occasional small clasts and lonestones (Kowallis and Craddock, 1984; Birkenmeijer, 2009, 2012; Bjørnerud 2010). Bjørnerud (2010) interpreted this as the outflow at the foot of a glacier bound by fast sea-ice until the final melting of the sea-ice allowed for formation of occasional icebergs, which deposited the dropstones found in the formation, until ultimately releasing large numbers of icebergs at a rate that deposited sediments that formed the upper massive diamictite observed in higher in the stratigraphy. To build up the 1000m of laminated sediment observed by these prior studies and the lack of accompanying carbonate unit, it would imply the sequence of deposition that formed the Kapp Lyell diamictites occurred in a deep basin, where as the thinner sediments of Kapp Linné imply that the deposition occurred more proximal to the shore, possibly in an outer shelf environment or along a topographic high. Overturning of the stratigraphy is possible. Viewed in reverse the Kapp Linné series fits the description of snowball Earth sequences laid out by Fairchild and Kennedy (2007) of a diamictite overlain by a cap carbonate which is then overlain by siltstone. No evidence of a reversed stratigraphy was observed at Kapp Linné, nor has it been observed in any of the Bellsund group to which the Kapp Linné series belongs (Kowallis and Craddock, 1984; Harland, Hambrey and Waddams, 1993) Birkenmeijer, 2009, 2012; Bjørnerud 2010). The correlation of the laminated diamictite at the base of both units is further evidence that there was no small scale overturning of the stratigraphy at Kapp Linné.

Therefore the following meltout and depositional regime is proposed.

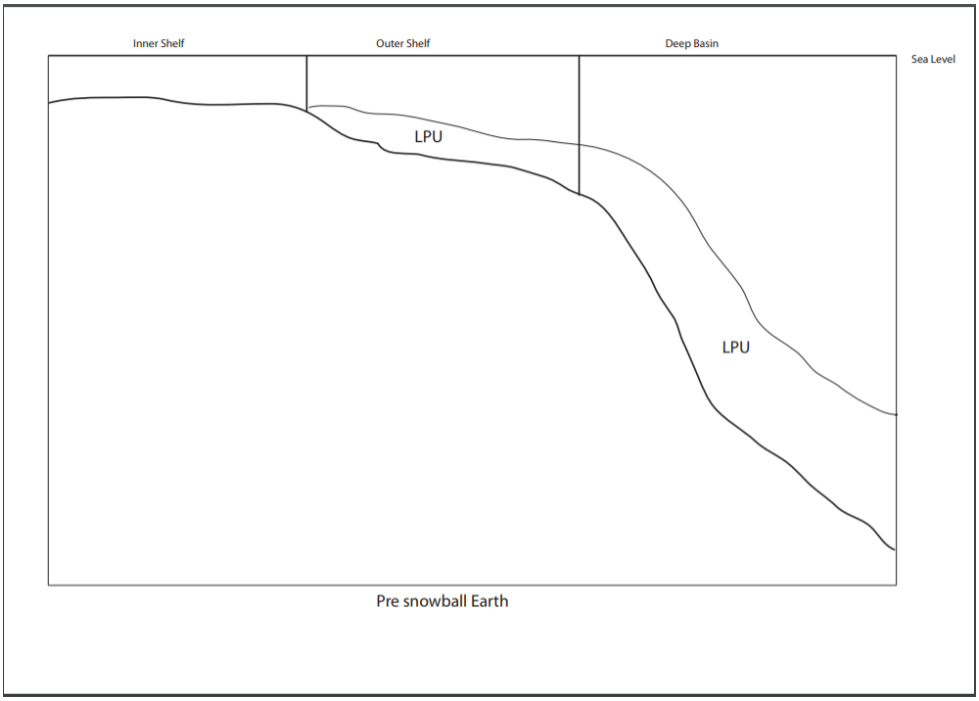


Stage 1. Kapp Linné is situated at an outer shelf depositional environment, where the LPU is deposited.

.

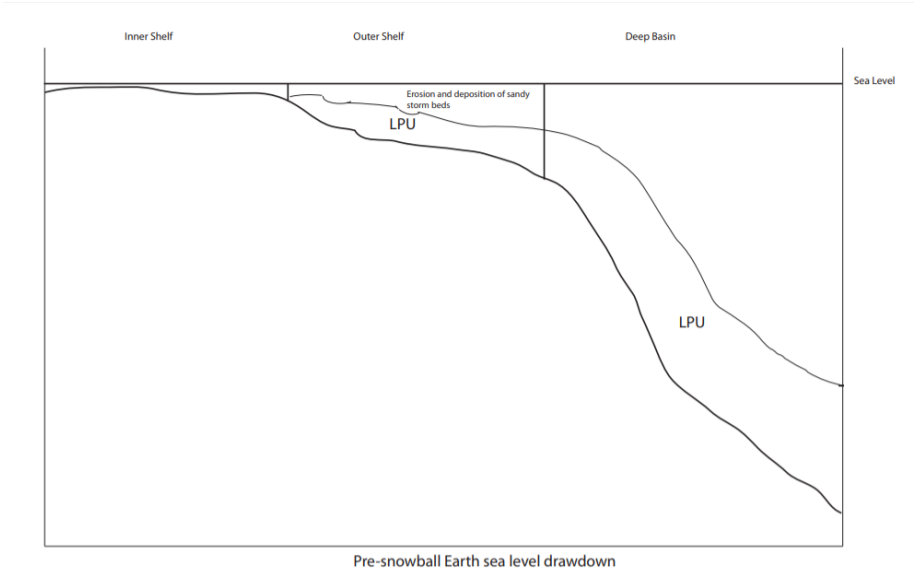


Stage 2. During the pre-snowball sea level drawdown, the LPU is shallower and is exposed to erosion during storms, leading to the sandy lenses at the top of the unit

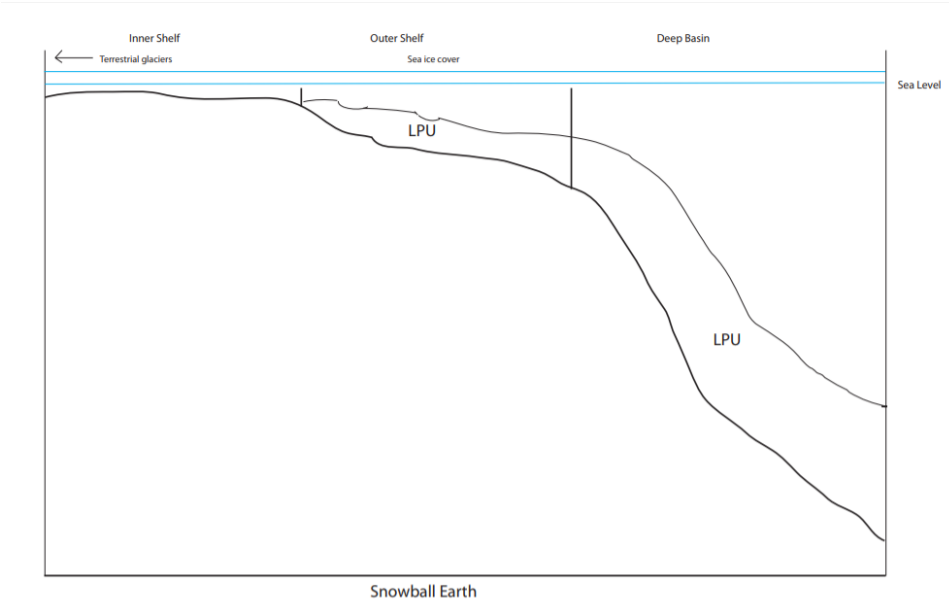


Stage 3. Snowball Earth. The area is covered by sea ice. The oceans become anoxic and Fe-Mn levels increase in the sea from hydrothermal activity

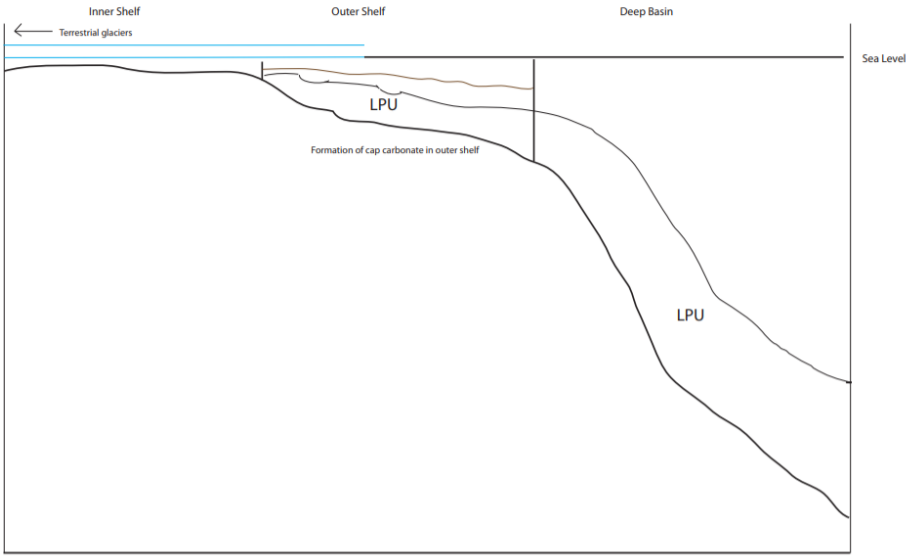


Stage 4. Meltdown.The sea ice melts, exposing the ocean to oxygen, reducing the Fe and Mn in the water, and triggering the precipitation of carbonate, forming the LCU.

.

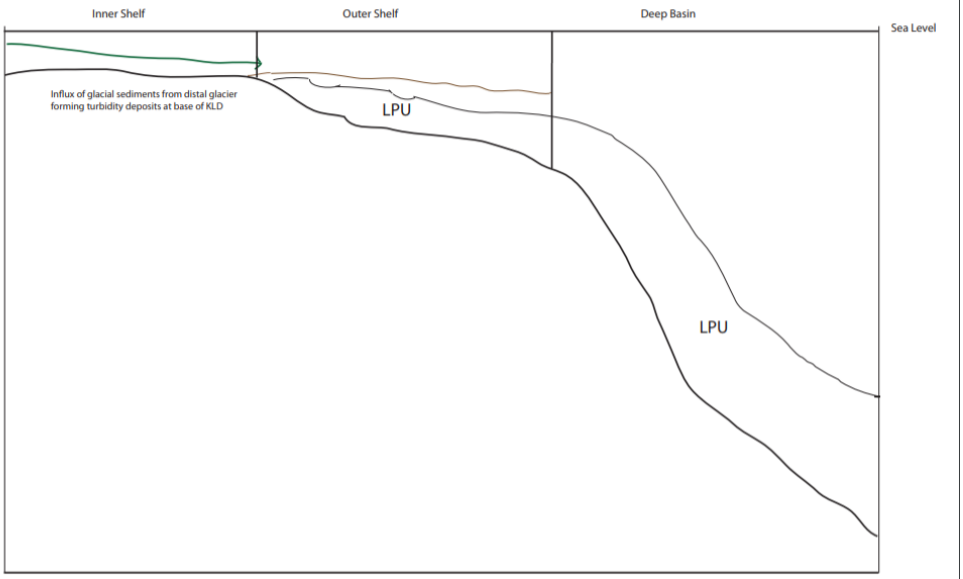


Stage 5. The melting of the glaciers has raised the sea levels and is beginning to deposit the turbidity deposits that form the bottom of the KLD

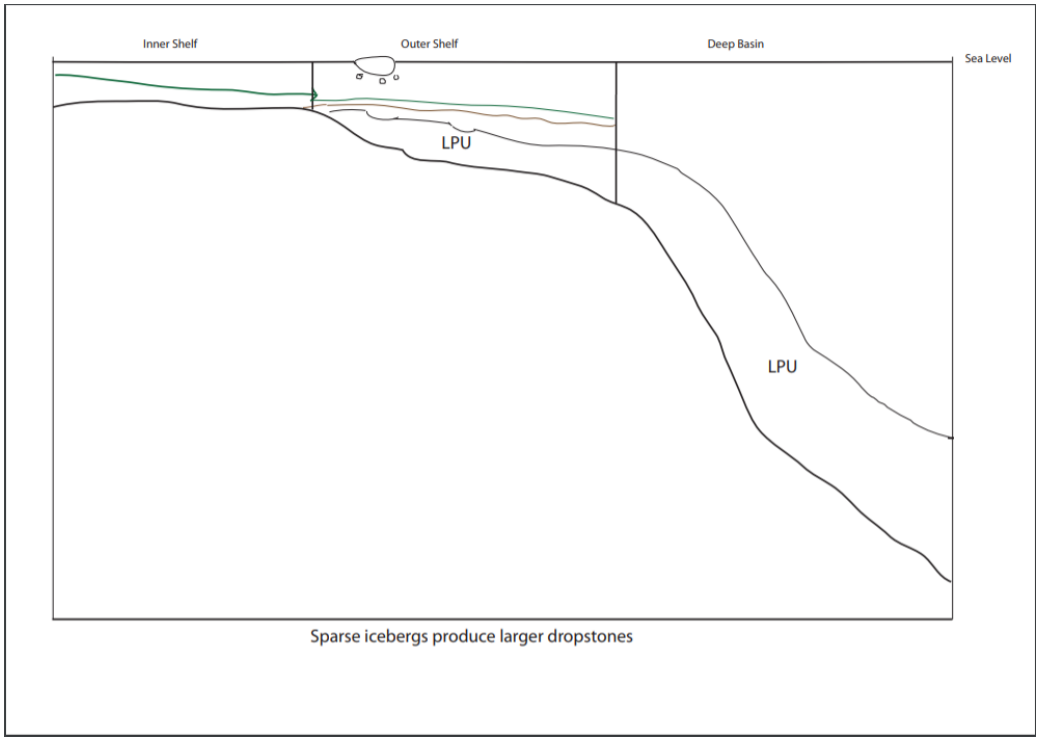


Stage 6. Sparse icebergs begin depositing the dropstones of the KLD.

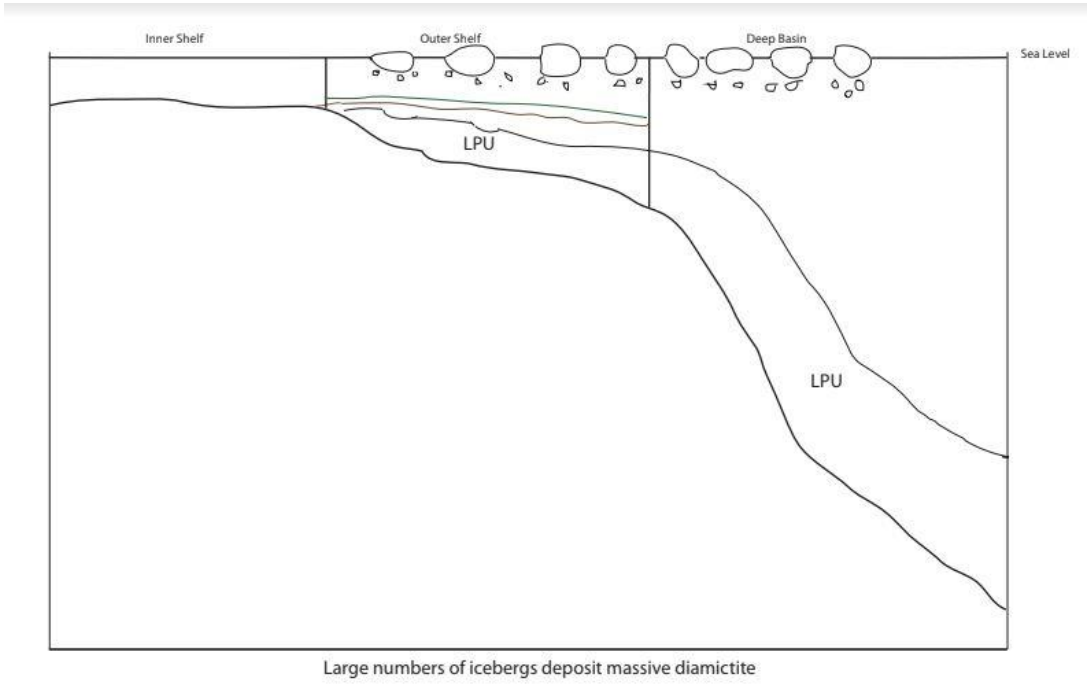


Stage 7. High levels of iceberg rafting deposits the massive diamictite

### Upper Carbonate Unit:

The UCU had a slightly lower $\delta^{13}C$ than the LCU, around .5‰ (see tables 5-10) higher FeO and MnO than the LCU. Additionally it lacks the lamination/foliation structures observed in the LCU (see the outcrop images in Fig. 28 and 24, and the thin sections in Fig. 29 and 25). This indicates that it is a separate unit likely deposited under different conditions. The formation of this unit may have occurred after the cessation of ice-rafting allowing the continued growth of the LCU, with the KLD truncating the growth. Further examination of the UCU will be conducted summer 2019 to better constrain the placement in the stratigraphy.

## Conclusions

The Kapp Linné series correlates to the Bellsund Group and Kapp Lyell diamictites, though the thinner beds indicated that these were deposited in a shallower basin possibly on a topographic high. The geochemistry of the stable isotopes from the carbonate units found at Kapp Linné show a transition from positive $\delta^{13}C$ values in the lowest carbonate unit to negative values in the uppermost carbonate unit, a classic sign of a "snowball" Earth deposit. Additionally the high values of Mn and Fe in the "cap" carbonate unit is evidence of the anoxic conditions under an ice covered sea at near equatorial paleo-latitudes, further evidence that the Kapp Linné formation originated in a snowball Earth scenario. Comparison of the major oxides at Kapp Linné show they have more in common with Sturtian cap carbonates, possibly pointing to an earlier deposition than previous work has estimated.

The positioning of a carbonate unit that fits the description of "cap" carbonates from other snowball Earth deposits around the world presents a challenge that this study has not been able to fully explain. The outer shelf in the vicinity of a marine topographic high in a rifting environment as presented is a possible explanation for the deposition of a carbonate unit below a glacio-marine diamictite with a second chemically and isotopically similar carbonate unit above the diamictite. Further investigation of Kapp Linné with a focus on the stratigraphy of these three units is needed to test this hypothesis and better understand the formation of these carbonate units.

## Acknowledgements

The author would like to thank the faculty of Stockholms Universitet, especially Alasdair Skelton, whose dedication to his students made this work possible, and Heike Sigmund for running the stable isotope tests. Thanks also go to the faculty and staff at the University Center in Svalbard, especially Maria Jensen for her help in planning the fieldwork, Tom Birchall who suffered frostbite while assisting in the collection of samples, and Sarah Cohen, who always got me where I was going safely.

## Works Cited:

Allen, P. A., & Etienne, J. L. (2008). Sedimentary challenge to snowball Earth. *Nature Geoscience*, *1*(12), 817.

Berner, R. A. (1978). Rate control of mineral dissolution under earth surface conditions. *American Journal of Science*, *278*(9), 1235-1252.

Birkenmajer, K. (2003). The Kapp Lyell diamictite (Late Proterozoic), Bellsund, Spitsbergen: sedimentological evidence for its non-glacial origin. *Bulletin of the Polish Academy of Sciences. Earth Sciences*, *51*(1), 65-78.

Bjornerud, M. (1989). Mathematical model for folding of layering near rigid objects in shear deformation. *Journal of Structural Geology*, *11*(3), 245-254.

Bjørnerud, M. (1990). An Upper Proterozoic unconformity in northern Wedel Jarlsberg Land, southwest Spitsbergen: lithostratigraphy and tectonic implications. *Polar Research*, *8*(2), 127-139.

Bjørnerud, M. G. (2010). Stratigraphic record of Neoproterozoic ice sheet collapse: the Kapp Lyell diamictite sequence, SW Spitsbergen, Svalbard. *Geological Magazine*, *147*(3), 380-390.

Caldeira, K., & Kasting, J. F. (1992). Susceptibility of the early Earth to irreversible glaciation caused by carbon dioxide clouds. *Nature*, *359*(6392), 226.

Crowley, T. J., Hyde, W. T., & Peltier, W. R. (2001). CO2 levels required for deglaciation of a "Near-Snowball" Earth. *Geophysical Research Letters*, *28*(2), 283-286.

Fairchild, I. J., & Hambrey, M. J. (1995). Vendian basin evolution in East Greenland and NE Svalbard. *Precambrian Research*, *73*(1-4), 217-233

Fairchild, I. J., Fleming, E. J., Bao, H., Benn, D. I., Boomer, I., Dublyansky, Y. V., ... & Spötl, C. (2016). Continental carbonate facies of a Neoproterozoic panglaciation, north-east Svalbard. *Sedimentology*, *63*(2), 443-497.

Fairchild, I. J., & Kennedy, M. J. (2007). Neoproterozoic glaciation in the Earth System. *Journal of the Geological Society*, *164*(5), 895-921.

Feng, F., Guan, P., Liu, W., Zhang, W., Liu, P., Jian, X., & Fu, L. (2016). Geochemistry of Altungol cap dolostones from the Tarim Basin, NW China. *Arabian Journal of Geosciences*, *9*(18), 715.

Ferry, J. M. (1987). Thermodynamic models of molecular fluids at the elevated pressures and temperatures of crustal metamorphism. *Thermodynamic Modeling of Geological Materials: Minerals, Fluids and Melts*, 323-365.

Font, E., Nédélec, A., Trindade, R. I. F., Macouin, M., & Charrière, A. (2006). Chemostratigraphy of the Neoproterozoic Mirassol d'Oeste cap dolostones (Mato Grosso, Brazil): an alternative model for Marinoan cap dolostone formation. *Earth and Planetary Science Letters*, *250*(1-2), 89-103.

Forman, S. L., & Ingolffson, Ó. (2000). Late Weichselian glacial history and postglacial emergence of Phippsøya, Sjuøyane, northern Svalbard: a comparison of modelled and empirical estimates of a glacial-rebound hinge line. *Boreas*, *29*(1), 16-25.

Franchi, F. (2018). Petrographic and geochemical characterization of the Lower Transvaal Supergroup stromatolitic dolostones (Kanye Basin, Botswana). *Precambrian Research*, *310*, 93-113.

Giddings, J. A., & Wallace, M. W. (2009). Sedimentology and C-isotope geochemistry of the 'Sturtian'cap carbonate, South Australia. *Sedimentary Geology*, *216*(1-2), 1-14.

Graf, D. L. (1960). Geochemistry of carbonate sediments and sedimentary carbonate rocks: pt. III, Minor element distribution. *Circular no. 301*.

Grotzinger, J. P., & Knoll, A. H. (1995). Anomalous carbonate precipitates: is the Precambrian the key to the Permian?. *Palaios*, 578-596.

Halverson, G. P., Hoffman, P. F., Schrag, D. P., & Kaufman, A. J. (2002). A major perturbation of the carbon cycle before the Ghaub glaciation (Neoproterozoic) in Namibia: Prelude to snowball Earth?. *Geochemistry, Geophysics, Geosystems*, *3*(6), 1-24.

Halverson, G. P., Maloof, A. C., & Hoffman, P. F. (2004). The Marinoan glaciation (Neoproterozoic) in northeast Svalbard. *Basin Research*, *16*(3), 297-324.

Halverson, G. P., Wade, B. P., Hurtgen, M. T., & Barovich, K. M. (2010). Neoproterozoic chemostratigraphy. *Precambrian Research*, *182*(4), 337-350.

Hambrey, M. J., & Harland, W. B. (Eds.). (2011). *Earth's pre-Pleistocene glacial record*. Cambridge University Press

Harland, W. B., Hambrey, M. J., & Waddams, P. (1993). Vendian geology of Svalbard.

Henderson-Sellers, A., & Wilson, M. F. (1983). Albedo observations of the earth's surface for climate research. *Philosophical Transactions of the Royal Society of London. Series A, Mathematical and Physical Sciences*, *309*(1508), 285-294.

Higgins, J. A., & Schrag, D. P. (2003). Aftermath of a snowball Earth. *Geochemistry, Geophysics, Geosystems*, *4*(3).

Hillaire-Marcel, Claude, and A. C. Ravelo. "The use of Oxygen and Carbon isotopes of Foraminifera in Paleoceanography." *Developments in Marine Geology: Proxies in Late Cenozoic Paleoceanography. Burlington: Elsevier Science* (2007).

Hoffman, P. F., Kaufman, A. J., Halverson, G. P., & Schrag, D. P. (1998). A Neoproterozoic snowball earth. *science*, *281*(5381), 1342-1346.

Hoffman, P. F., & Schrag, D. P. (2002). The snowball Earth hypothesis: testing the limits of global change. *Terra nova*, *14*(3), 129-155.

Hoffman, P. F., Abbot, D. S., Ashkenazy, Y., Benn, D. I., Brocks, J. J., Cohen, P. A., ... & Fairchild, I. J. (2017). Snowball Earth climate dynamics and Cryogenian geology-geobiology. *Science Advances*, *3*(11), e1600983.

Hyde, W. T., Crowley, T. J., Baum, S. K., & Peltier, W. R. (2000). Neoproterozoic 'snowball Earth' simulations with a coupled climate/ice-sheet model. *Nature*, *405*(6785), 425.

James, N. P., Narbonne, G. M., & Kyser, T. K. (2001). Late Neoproterozoic cap carbonates: Mackenzie Mountains, northwestern Canada: precipitation and global glacial meltdown. *Canadian Journal of Earth Sciences*, *38*(8), 1229-1262.

Jiang, G., Kennedy, M. J., & Christie-Blick, N. (2003). Stable isotopic evidence for methane seeps in Neoproterozoic postglacial cap carbonates. *Nature*, *426*(6968), 822.

Johansson, Å., Gee, D. G., Larionov, A. N., Ohta, Y., & Tebenkov, A. M. (2005). Grenvillian and Caledonian evolution of eastern Svalbard–a tale of two orogenies. *Terra Nova*, *17*(4), 317-325.

Kaminskas, D., Bickauskas, G., & Brazauskas, A. (2010). Silurian dolostones of eastern Lithuania. *Estonian Journal of Earth Sciences*, *59*(2).

Kennedy, M. J., Christie-Blick, N., & Sohl, L. E. (2001). Are Proterozoic cap carbonates and isotopic excursions a record of gas hydrate destabilization following Earth's coldest intervals?. *Geology*, *29*(5), 443-446.

Kennedy, M. J., & Christie-Blick, N. (2011). Condensation origin for Neoproterozoic cap carbonates during deglaciation. *Geology*, *39*(4), 319-322.

Khalaf, F. I., Abdullah, F. A., & Gharib, I. M. (2018). Petrography, diagenesis and isotope geochemistry of dolostones and dolocretes in the Eocene Dammam Formation, Kuwait, Arabian Gulf. *Carbonates and Evaporites*, *33*(1), 87-105.

Kowallis, B. J., & Craddock, C. (1984). Stratigraphy and structure of the Kapp Lyell diamictites (upper Proterozoic), Spitsbergen. *Geological Society of America Bulletin*, *95*(11), 1293-1302.

Krasil'scikov, A. A. (1979). Stratigraphy and tectonics of the Precambrian of Svalbard. *Norsk Polarinstitutt Skrifter*, *167*, 73-79.

Li, Z. X., Bogdanova, S. V., Collins, A. S., Davidson, A., De Waele, B., Ernst, R. E., ... & Karlstrom, K. E. (2008). Assembly, configuration, and break-up history of Rodinia: a synthesis. *Precambrian research*, *160*(1-2), 179-210.

Li, Zheng-Xiang, David AD Evans, and Galen P. Halverson. "Neoproterozoic glaciations in a revised global palaeogeography from the breakup of Rodinia to the assembly of Gondwanaland." *Sedimentary Geology* 294 (2013): 219-232.

Lumsden, D. N., & Caudle, G. C. (2001). Origin of massive dolostone: the Upper Knox model. *Journal of Sedimentary Research*, *71*(3), 400-409.

McKirdy, D. M., Burgess, J. M., Lemon, N. M., Yu, X., Cooper, A. M., Gostin, V. A. Jenkins & Both, R. A. (2001). A chemostratigraphic overview of the late Cryogenian interglacial sequence in the Adelaide Fold-Thrust Belt, South Australia. *Precambrian Research*, *106*(1-2), 149-186.

Meyer, E. E., Quicksall, A. N., Landis, J. D., Link, P. K., & Bostick, B. C. (2012). Trace and rare earth elemental investigation of a Sturtian cap carbonate, Pocatello, Idaho: evidence for ocean redox conditions before and during carbonate deposition. *Precambrian Research*, *192*, 89-106.

Mazur, S., Czerny, J., Majka, J., Manecki, M., Holm, D., Smyrak, A., & Wypych, A. (2009). A strike-slip terrane boundary in Wedel Jarlsberg Land, Svalbard, and its bearing on correlations of SW Spitsbergen with the Pearya terrane and Timanide belt. *Journal of the Geological Society*, *166*(3), 529-544.

Pollard, D., & Kasting, J. F. (2005). Snowball Earth: A thin-ice solution with flowing sea glaciers. *Journal of Geophysical Research: Oceans*, *110*(C7).

Rose, C. V., Swanson-Hysell, N. L., Husson, J. M., Poppick, L. N., Cottle, J. M., Schoene, B., & Maloof, A. C. (2012). Constraints on the origin and relative timing of the Trezona δ13C anomaly below the end-Cryogenian glaciation. *Earth and Planetary Science Letters*, *319*, 241-250.

Shields, G. A. (2005). Neoproterozoic cap carbonates: a critical appraisal of existing models and the plumeworld hypothesis. *Terra Nova*, *17*(4), 299-310.

Waddams, P. (1983). The late Precambrian succession in north-west Oscar II land, Spitsbergen. *Geological Magazine*, *120*(3), 233-252.

Whitney, D. L., & Evans, B. W. (2010). Abbreviations for names of rock-forming minerals. *American mineralogist*, *95*(1), 185-187.

Wilson, C. B., & Harland, W. B. (1964). The Polarisbreen Series and other evidences of late Pre-Cambrian ice ages in Spitsbergen. *Geological Magazine*, *101*(3), 198-219.

Xiao, S., Bao, H., Wang, H., Kaufman, A. J., Zhou, C., Li, G., ... & Ling, H. (2004). The Neoproterozoic Quruqtagh Group in eastern Chinese Tianshan: evidence for a post-Marinoan glaciation. *Precambrian Research*, *130*(1-4), 1-26.